Transport transforms for signal analysis and machine learning: applications

Gustavo K. Rohde

Imaging and Data Science Laboratory

imagedatascience.com/transport
github.com/rohdelab/PyTransKit

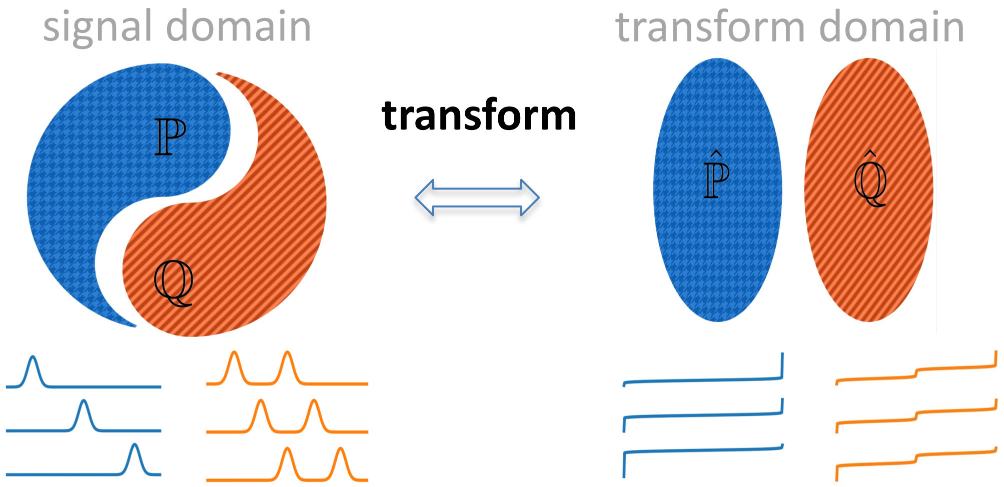

Fourier transform:

forward

$$\hat{s}(\omega) = \int s(t) e^{-jwt} dt$$

inverse

$$s(t) = \frac{1}{2\pi} \int \hat{s}(\omega) e^{k\omega t} d\omega$$

$$\int s(u) h(t-u) du = f(t)$$

signal domain

difficult to solve

$$\hat{s}(\omega)\hat{h}(\omega) = \hat{f}(\omega)$$

$$\hat{s}(\omega) = \hat{f}(\omega)/\hat{h}(\omega)$$

transform domain

easier to solve

$$s$$

signal domain

New signal transform:

CDT,
SCDT
R-CDT
LOT

forward

$$\hat{s}(x) := S^{-1}(x)$$

inverse

$$s(t) = \frac{d}{dt}(\hat{s})^{-1}$$

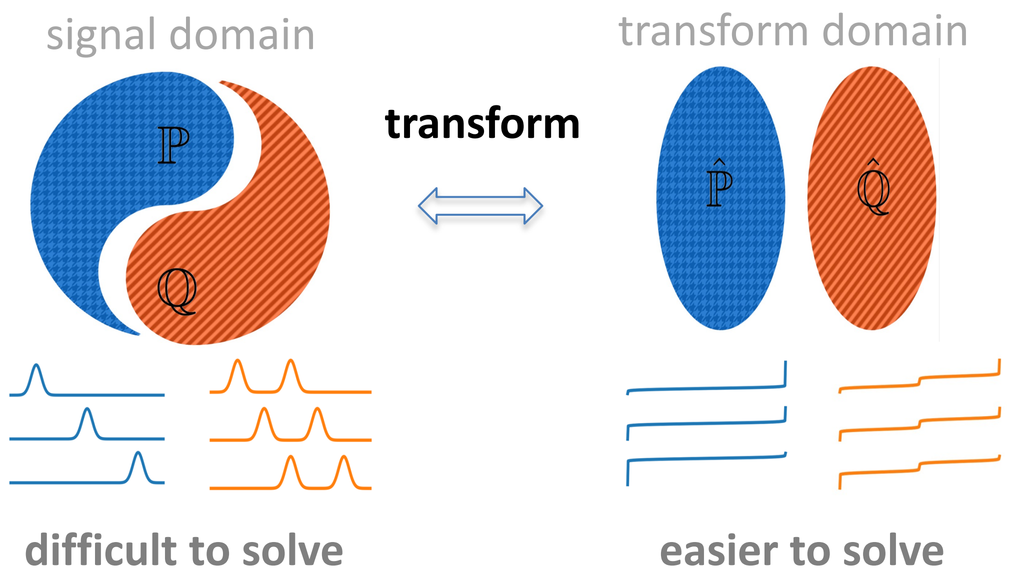

Summary: Transport & other Lagrangian Transforms

Nonlinear signal transform

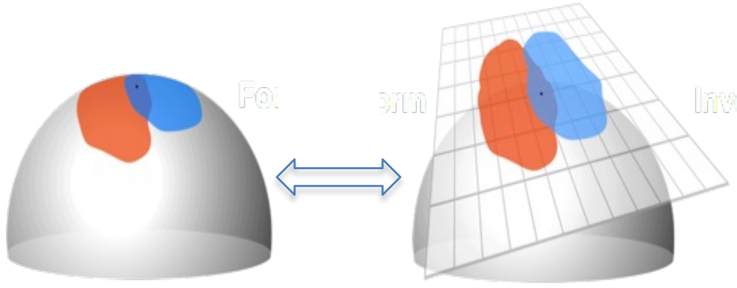

smooth PDFs　　diffeomorphisms

(LOT, CDT, R-CDT):

invertible transform framework for
Lagrangian modeling of signals & images
Connections to optimal transport

Properties

nonconvex,
nonlinear

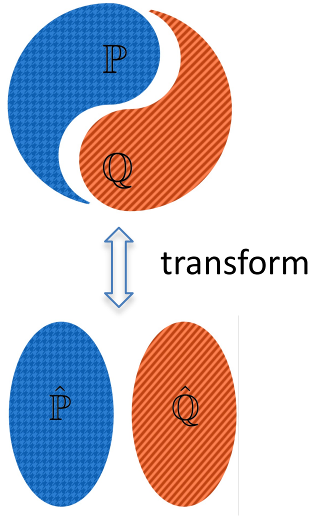

convex,
linearly separable

Intuition

Euclidean geodesics

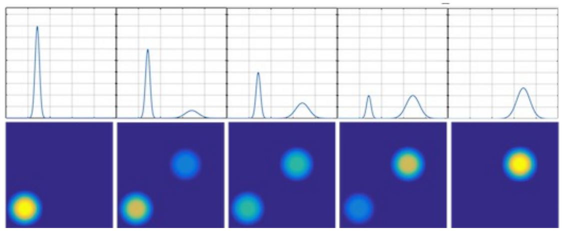

Transport geodesics

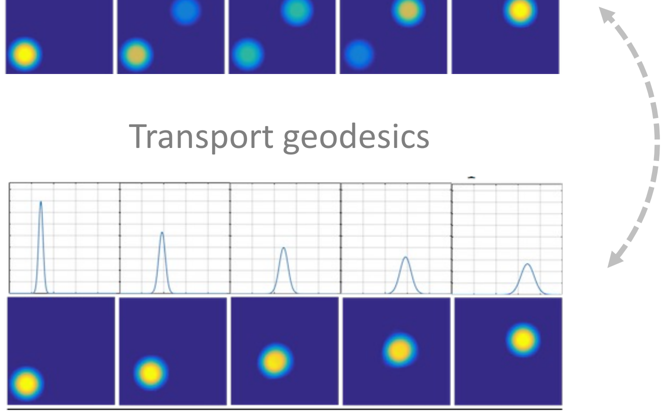

"looks around,"
moves intensities

Imagedatascience.com/transport

Topics covered

- Optimal transport overview
- Representing signals/images with transport transform/embeddings
- Applications
  - Nonlinear signal estimation
  - Model-based inverse problems
  - Transport-based morphometry (TBM)
  - Machine learning (e.g. classification)
- Summary

Outline

- Motivation
  - Transport-like processes
  - Nonlinear systems
- Estimation
  - Model training, parameter estimation
  - Inverse problems
- Transport-based morphometry
  - Cells, tissues, organs, faces, communications
  - Classification

Motivation

Model for signal/image deformations (transportations)

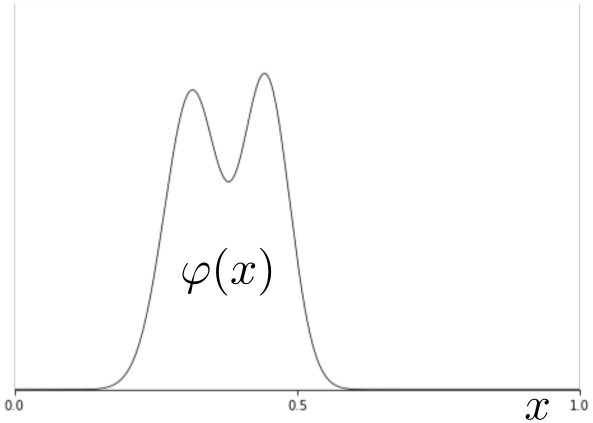

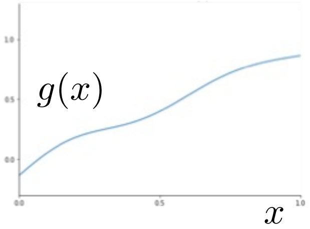

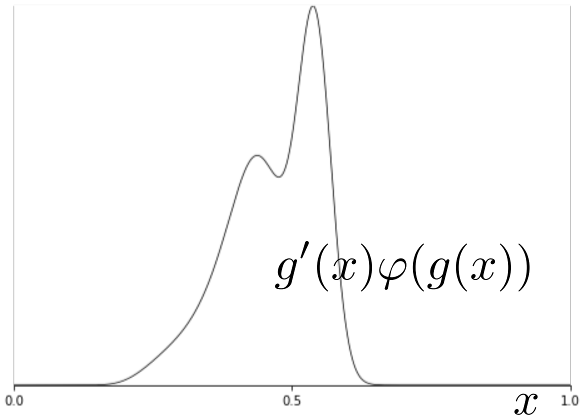

$\varphi(x)$

$g(x)$

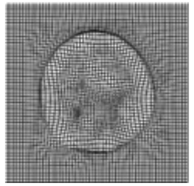

$x \in \Omega$

$D_g(x)\varphi(g(x))$

Translation:

$$g(x) = x - \tau$$

Scaling:

$$g(x) = ax$$

Nonrigid deformations:

$$g(x) = \sum_k c_k \phi_k(x)$$

What processes change signal/pixel intensity over time?

actin

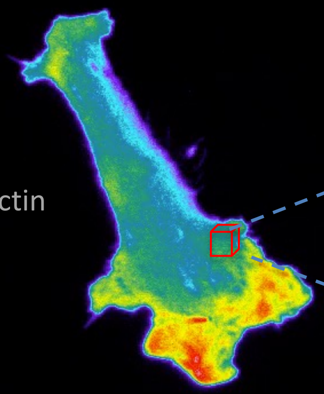

Johnson et al, JCB, 2015

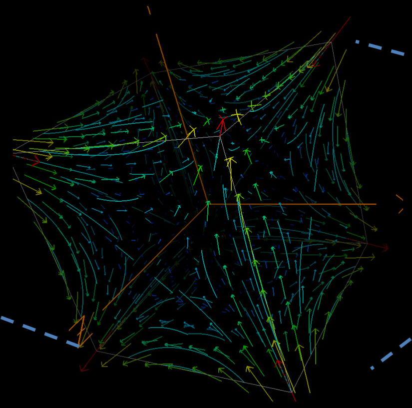

$\mathbf{v}$ flow/velocity

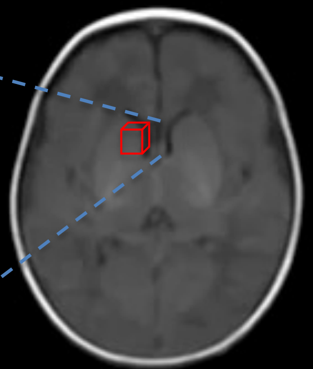

0 – 48 months

Nist lab, MNI

intensities not absolute

continuity equation

$$\underbrace{\frac{dI(x,y,z,t)}{dt}}_{\text{change in intensity at particular location}} = \underbrace{-\nabla \cdot (I(x,y,z,t)\mathbf{v}(x,y,z,t))}_{\text{net flux tissue velocity}} + \underbrace{\cancel{\ldots(I, \ldots y, \ldots t)}}_{\text{source/sink term}}$$

Transport with least action (optimal transport)

$$I(x,0) = I_0(x)$$
$$I(x,1) = I_1(x)$$

sample images
in a dataset

$$\frac{dI(x,t)}{dt} = -\nabla \cdot (I(x,y)v(x,t))$$

implies

$$I(x,t) = D_f(x) I_0(f(x,t))$$
$$f(x,t) = \int_0^t v(x,t)dt$$

Theorem: [Benamou, Brenier, Numer. Math, 2000]

$$W^2(I_0, I_1) = \inf_v \int_0^1 \int_\Omega I(x,t)|v(x,t)|^2 dxdt$$
$$f(x,t) = (1-t)x + t\nabla\phi$$

gradient of
convex function

Modeling light propagation in turbulence

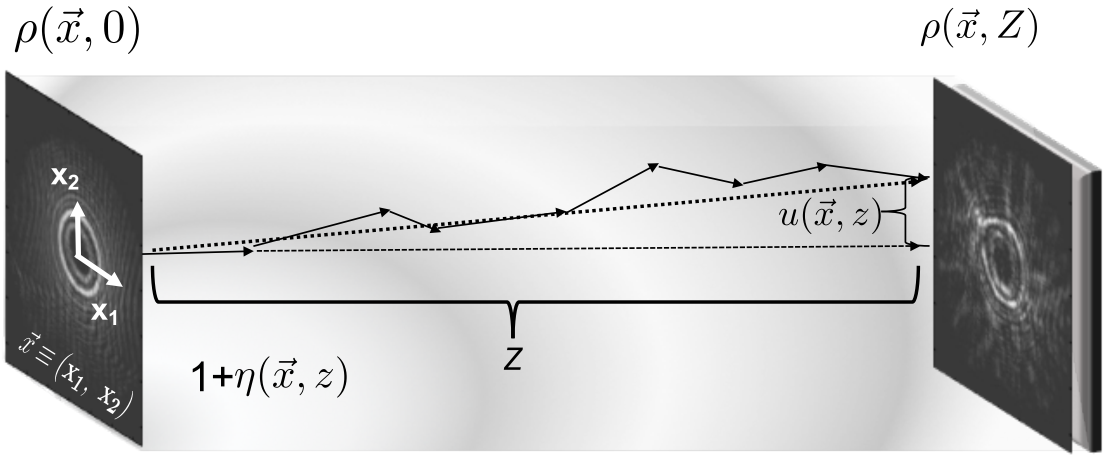

Light propagation path under turbulence

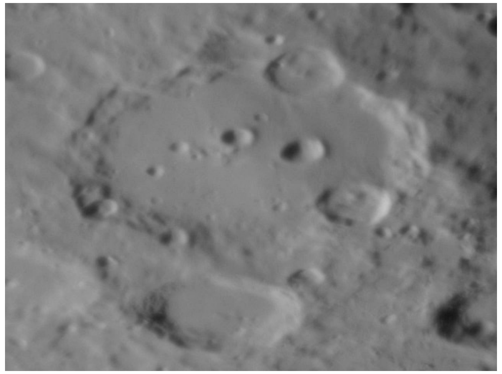

$$\frac{\partial \rho(\vec{x}, z)}{\partial z} + \nabla_X \cdot (\rho(\vec{x}, z) v(\vec{x}, z)) = 0$$ **Continuity eq.**

$$\frac{\partial v(\vec{x}, z)}{\partial z} + (v(\vec{x}, z) \cdot \nabla_X) v(\vec{x}, z) = 2\nabla_X g(\eta(\vec{x}, z)).$$ **Momentum eq.**

$\rho(\vec{x}, z)$: magnitude of the EM field
$v(\vec{x}, z)$: velocity in the transverse plane
$u(\vec{x}, z)$: displacement in transverse plane
$\eta(\vec{x}, z)$: refractive index

Nichols, Emerson, Rohde, Journal of Modern Optics, 2019.
Nichols, Emerson, Cattell, Park, Kanaev, Bucholtz, Watnik, Doster, GK Rohde, Applied Optics, 2018

Model/parameter estimation

Parametric signal estimation

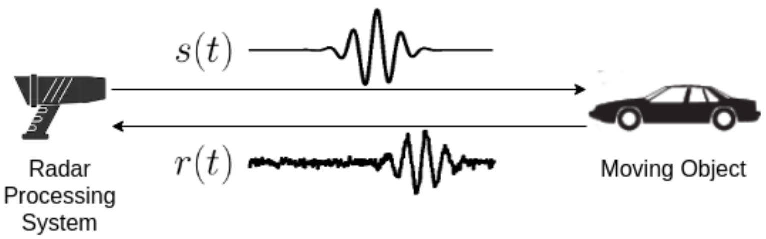

Static object: $r(t) = s(t-\tau) + \eta(t)$

Moving object: $r(t) = s(\omega t - \tau) + \eta(t)$

$g_p(t) = \omega t - \tau$

Traditional approach:

$$A_{r,s}(\tau,\omega) = \sqrt{\omega}\int r(t)s(\omega t - \tau)dt$$

$$\arg\min_{\tau,\omega} -|A_{r,s}(\tau,\omega)|$$

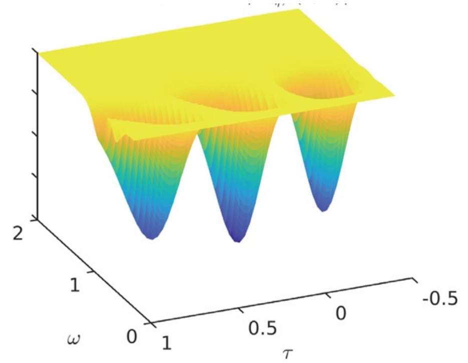

computationally expensive
global optimization required

Wasserstein minimization

$$W^2(r,s) = \|\omega\hat{r} - \tau - \hat{s}\|^2$$

$$\arg\min_{\tau,\omega} \|\omega\hat{r} - \tau - \hat{s}\|^2$$

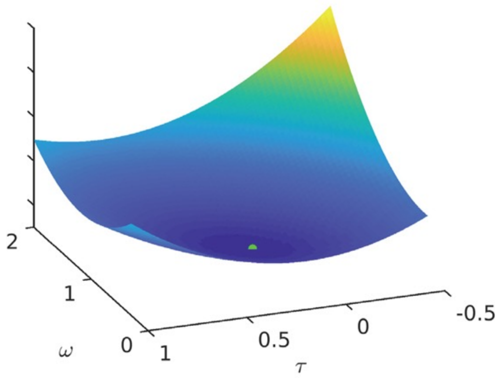

linear least squares
cheap to compute

AHM Rubaiyat, KM Hallam, JM Nichols, MN Hutchinson, S Li, GK Rohde, Parametric Signal Estimation Using the Cumulative Distribution Transform, IEEE Trans. Signal Processing, 68, pp. 3312-3324, 2020.

Parametric signal estimation

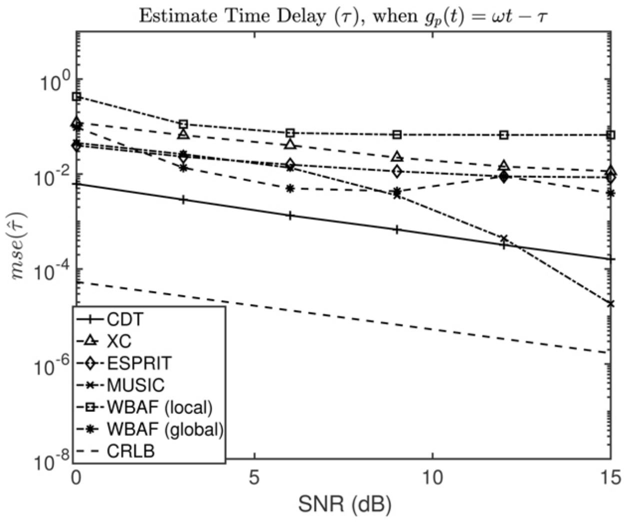

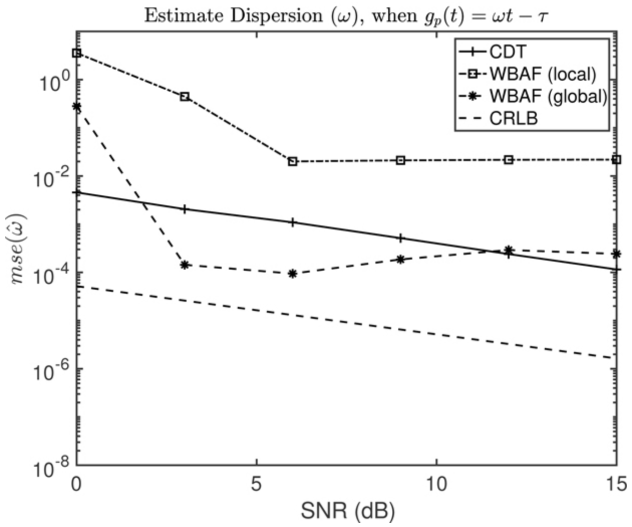

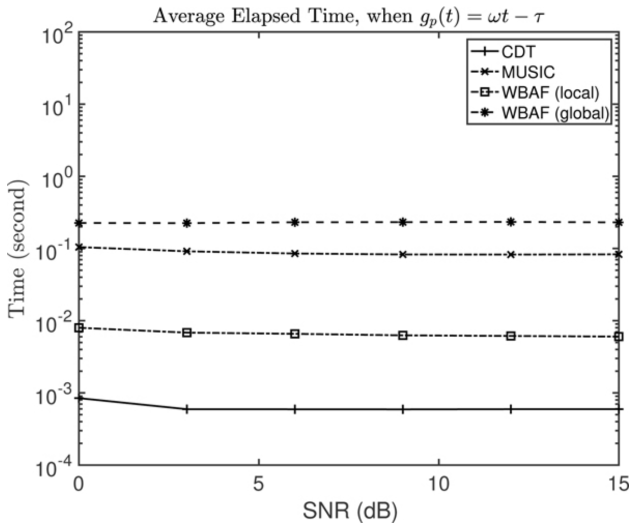

orders of magnitude cheaper to compute

AHM Rubaiyat, KM Hallam, JM Nichols, MN Hutchinson, S Li, GK Rohde, Parametric Signal Estimation Using the Cumulative Distribution Transform, IEEE Trans. Signal Processing, 68, pp. 3312-3324, 2020.

Parametric signal estimation in structural health monitoring

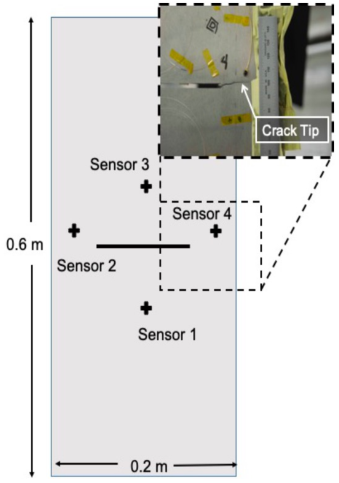

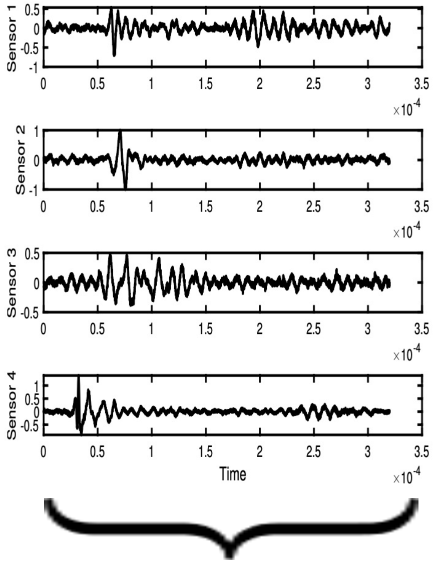

Estimate TDOA in CDT domain

Crack localization

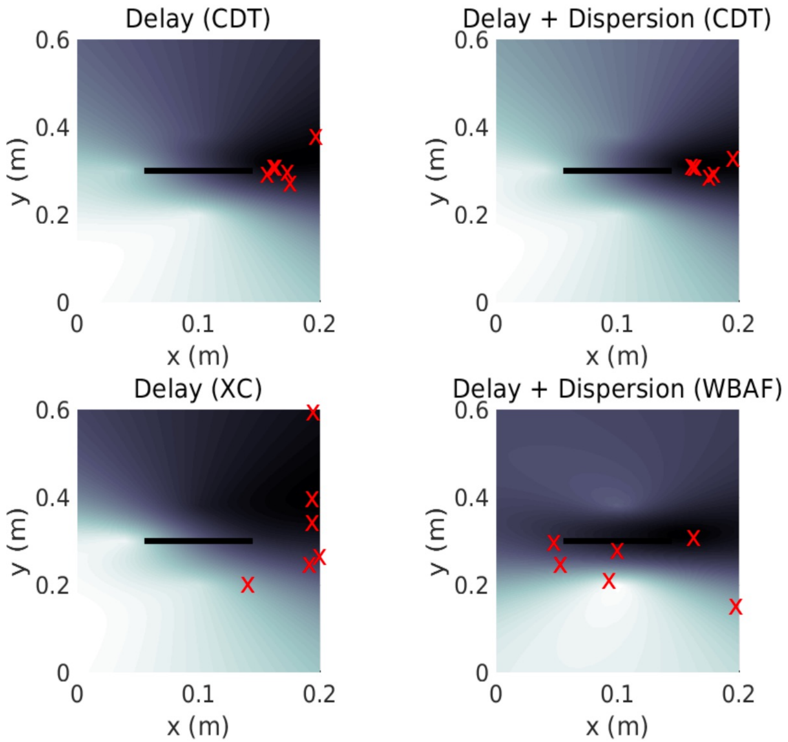

AHM Rubaiyat, KM Hallam, JM Nichols, MN Hutchinson, S Li, GK Rohde, Parametric Signal Estimation Using the Cumulative Distribution Transform, IEEE Trans. Signal Processing, 68, pp. 3312-3324, 2020.

Model-based inverse problems

Enhancing an image

Find model parameters that best match data

Random low resolution image of a crowd

Low resolution face

Reconstructed high resolution face

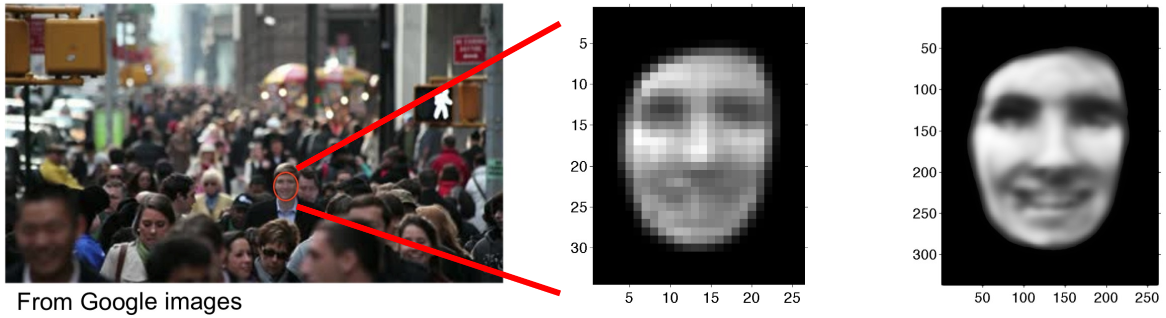

From Google images

Modeling phase

sample database

transform

PCA

model

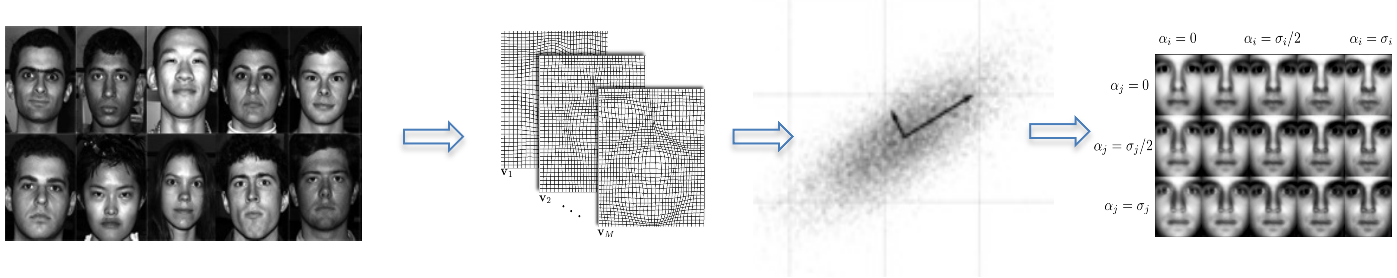

Application: single image super resolution

[Kolouri, Rohde, CVPR 2015]

Model: $$M_\alpha = D_{f_\alpha}(x) I_0(f_\alpha(x)) \qquad f_\alpha(x) = \underbrace{\sum_k \alpha_k \phi_k(x)}_{\text{Transport PCA trained on high res database}}$$

low-res data

Fit: $$\min_\alpha \|I - V M_\alpha\|^2$$

degradation

5x6 pixels!

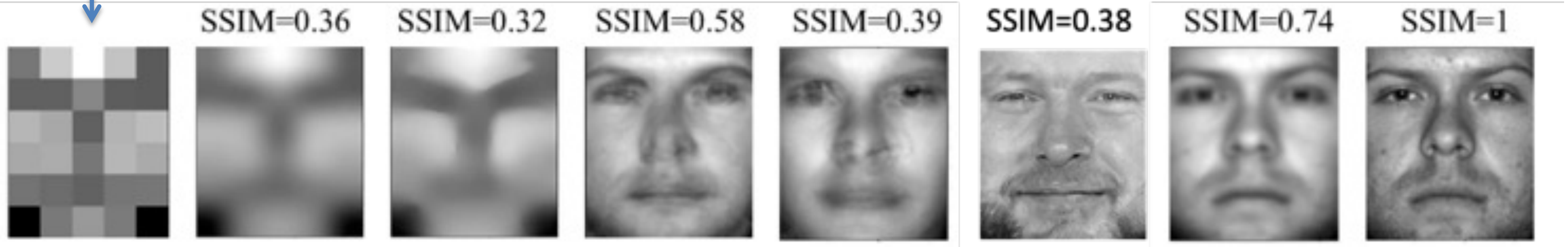

Input low-res data | B-spline interp. | compressed sensing | K-means nonlinear mapping | Kernel PCA | PULSE generative modeling | transport method | ground truth

Application: real time cardiac MRI

Radial K-space FBP-recon. Desired

Real time:

few K-space lines

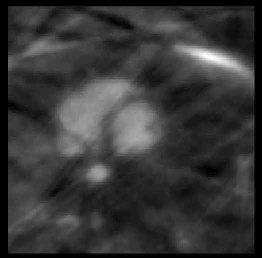

$\neq$

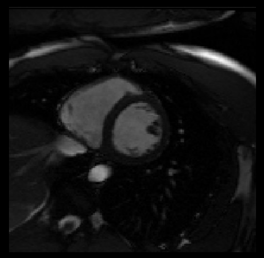

FBP Demons SparseMRI Proposed High-res

N = 21

N = 8

N = 2

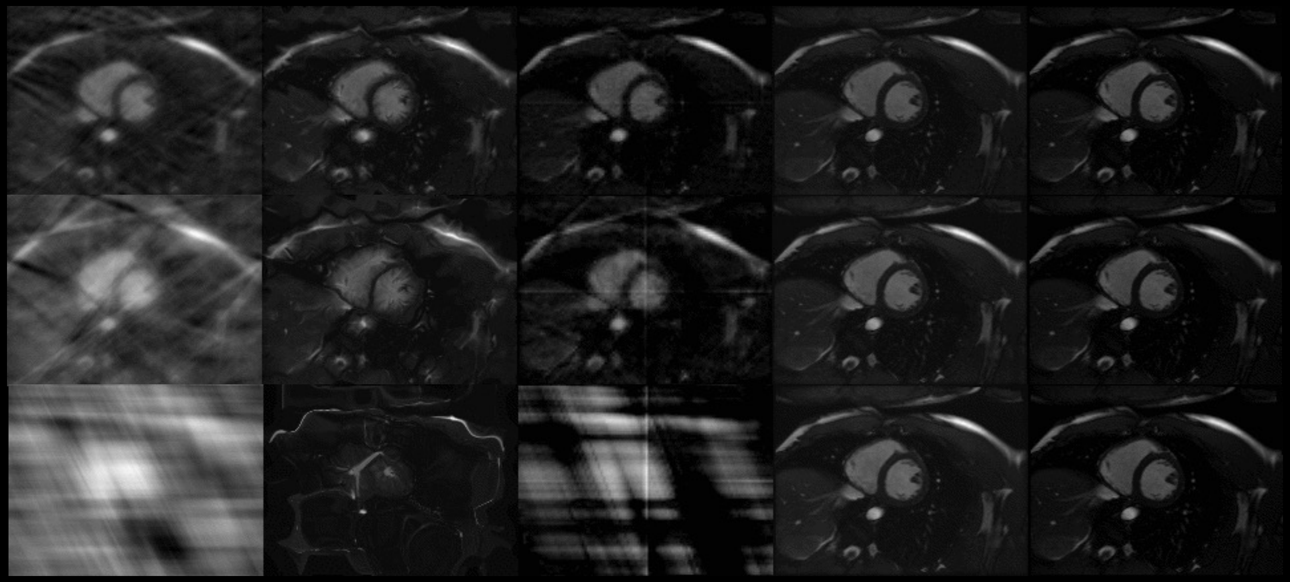

[Cattell, Meyer, Epstein, Rohde, IEEE Asilomar 17]

Transport-based Morphometry (TBM)

Biomedical image data science

Are fitness and gray matter morphology related?

Class 1:
persons with low fitness index

Class 2:
persons with high fitness index

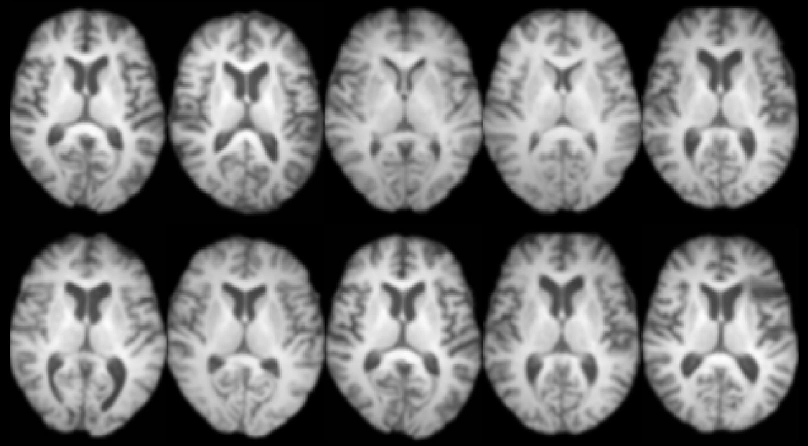

magnetic resonance imaging (MRI)

Hypothesis testing

Are there differences?

Understanding

If so, can we model them?

Is nuclear morphology related to cancer?

Class 1:
nuclei from benign tissues

Class 2:
nuclei from malignant tissues

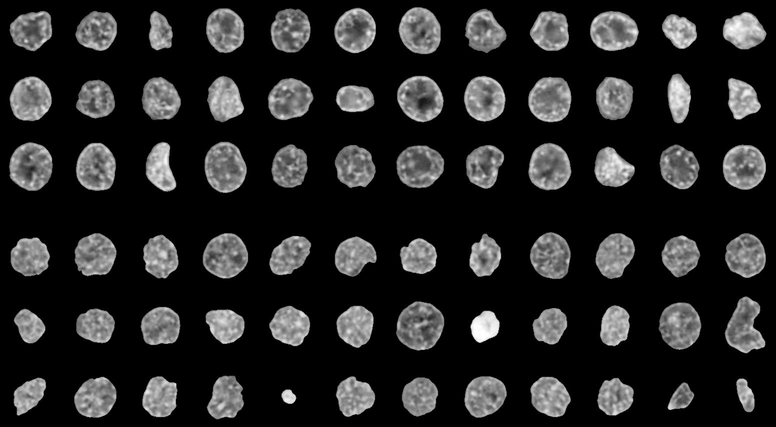

digital pathology (microscopy)

Transport-based morphometry (TBM)

1) Transform

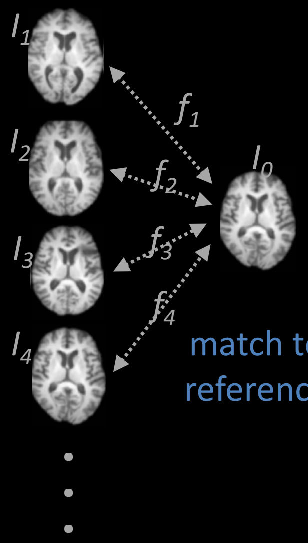

match to reference

transport maps

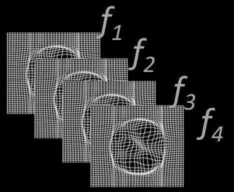

2) regression

modeling variations

- PCA, least squares, …

modeling differences

- LDA, SVM, …

modeling relationships

- CCA, …

3) Inverse transform

PCA, LDA, CCA, …

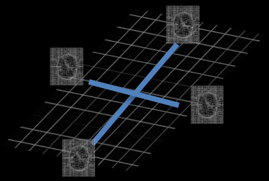

visualization

statistical regression (PCA, LDA, CCA, …)

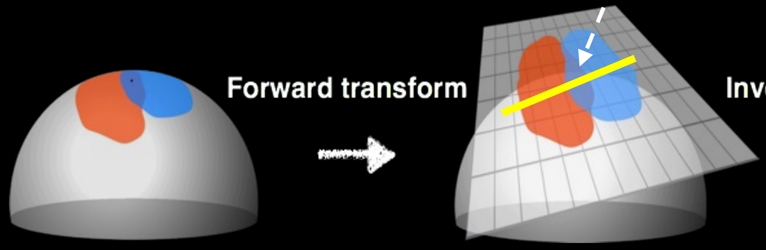

signal space

transform space

model in image space

Example: nuclear structure in cancer

Aberrations in genetic code and/or increase in transcriptional activity → Unfolding/repackaging of chromatin → change in nuclear configuration

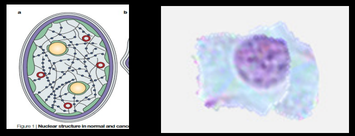

normal

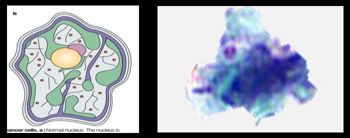

cancer

Pathology, whole slide imaging

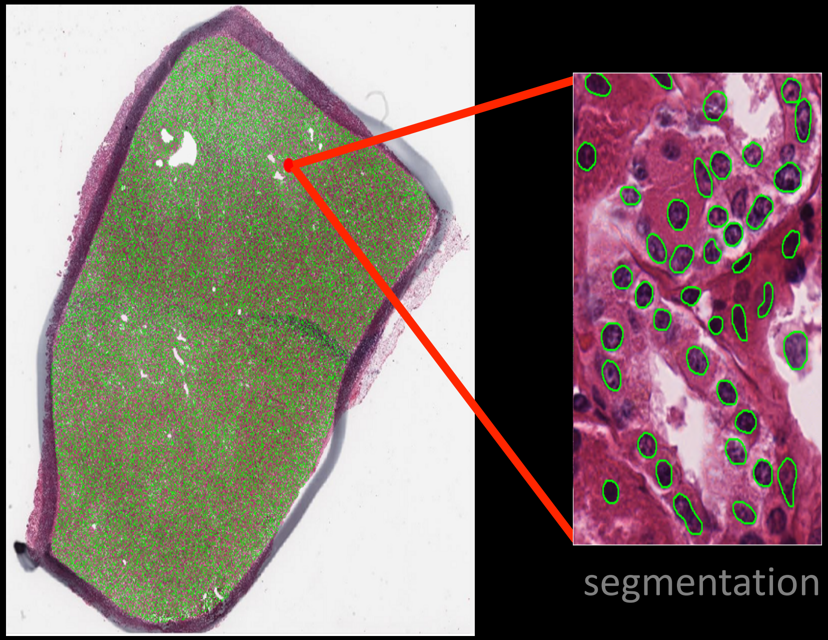

segmentation

→

segmented nuclei

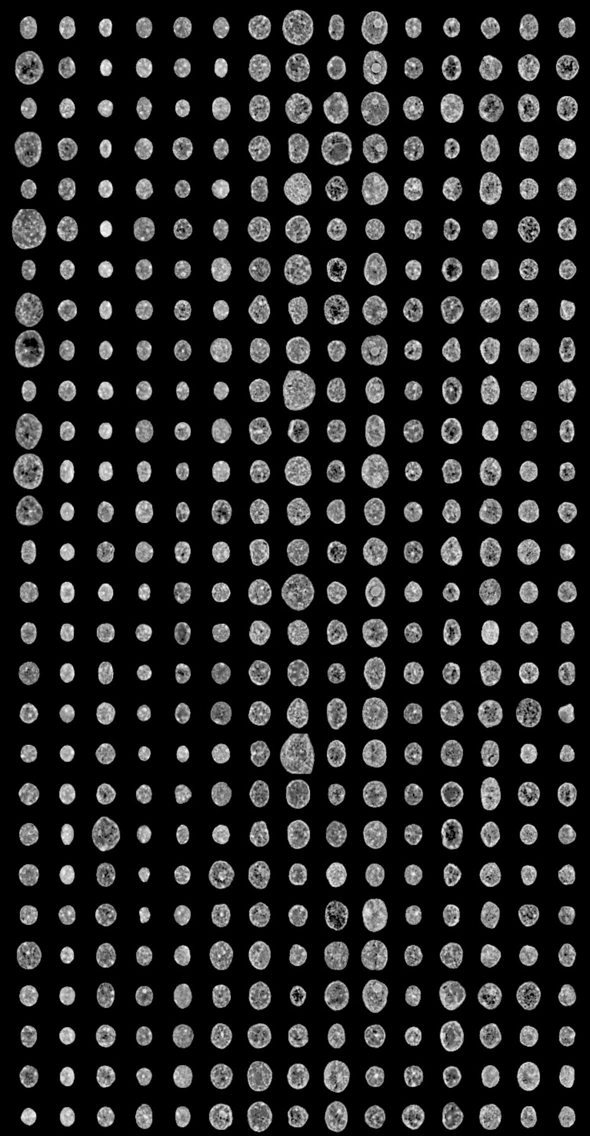

Exploratory analysis: PCA on transport maps

database

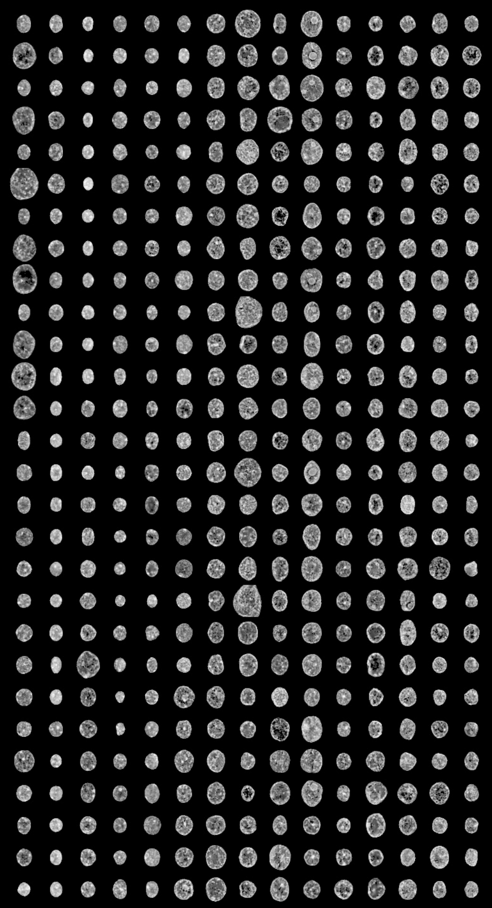

Modeling chromatin variation in liver cancer (shape + texture)

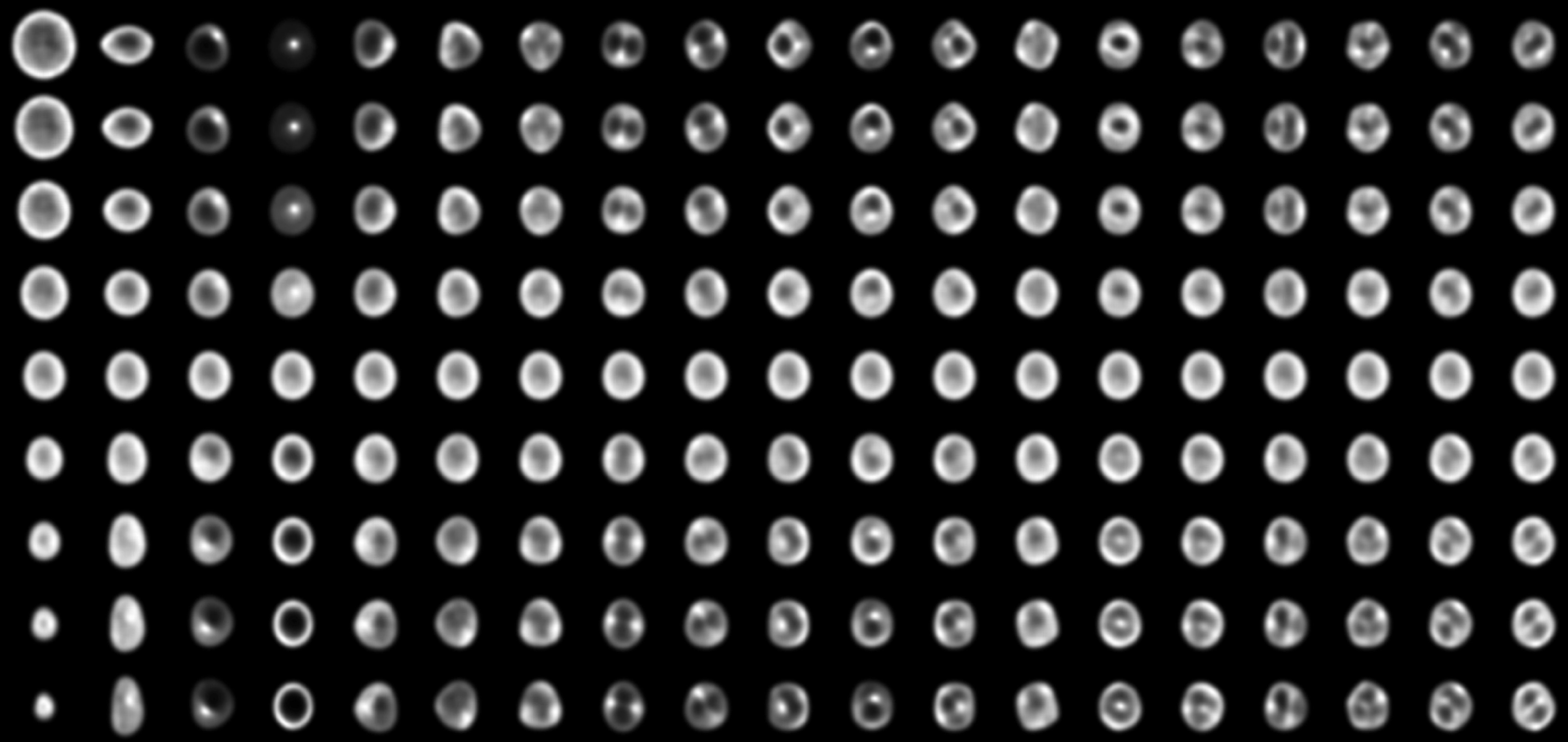

learned “features”

$$D_{f_\alpha^{-1}}(x)\, s_0(f_\alpha^{-1}(x))$$

$$f_\alpha(x) = \underbrace{f(x)}_{\text{mean}} + \alpha w(x)$$

PCA eigenvector

TBM: modeling discriminant information

[Basu et al, PNAS 2014]

Class 1: benign cells

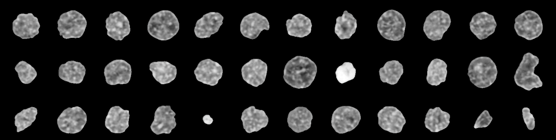

Class 2: malignant cells

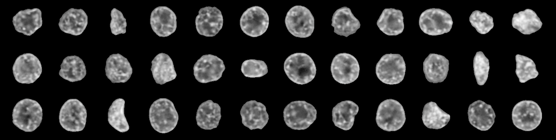

forward

LDA in transport space

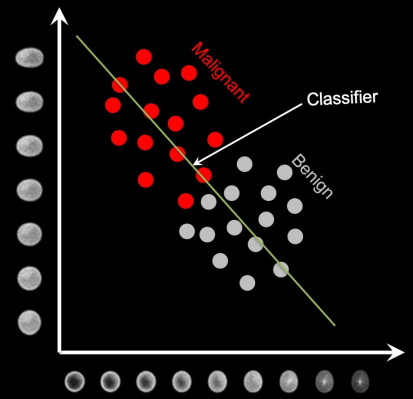

inverse

Fetal-type hepatoblastoma

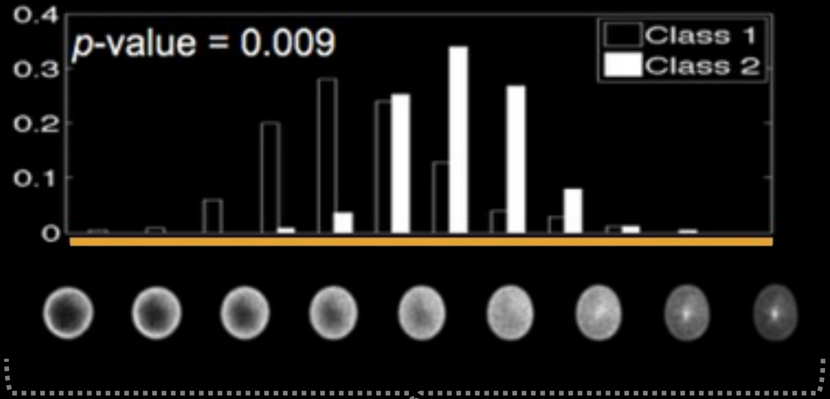

Inverse of classification function

$$D_{f_\alpha^{-1}}(x) s_0(f_\alpha^{-1}(x))$$

$$f_\alpha(x) = f(x) + \alpha w(x)$$

mean

classifier

TBM in early detection of osteoarthritis (OA)

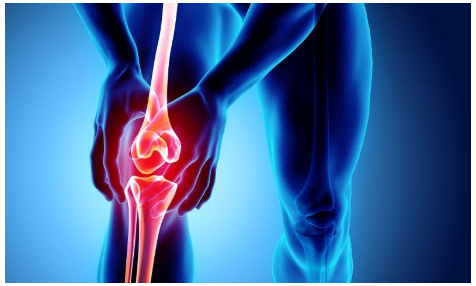

- OA affects 1 in 4 adults.
- Today OA is diagnosed at an irreversible stage.
- Diagnosis requires X-ray confirmation of bone damage.
- Early detection could prevent further development of disease.
- Early detection could stratify patient populations for treatment discovery.

T2-MRI of knee cartilage

- water molecules
- proteoglycans
- orientation of collagen fibers

medial femoral cartilage

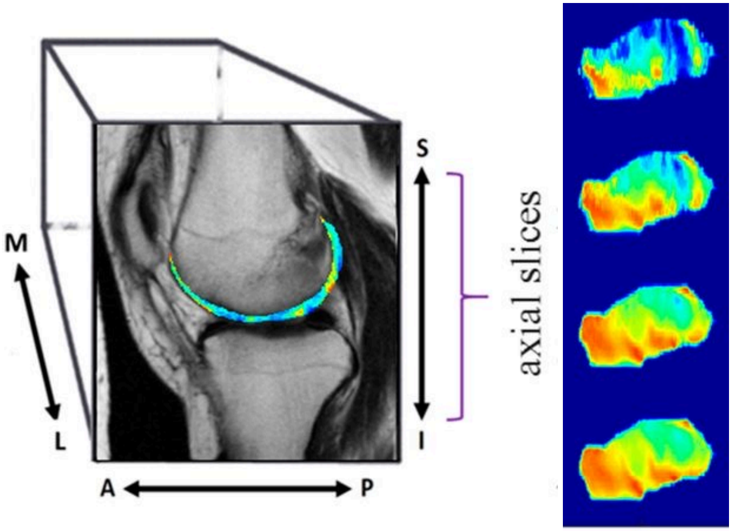

medial tibial cartilage

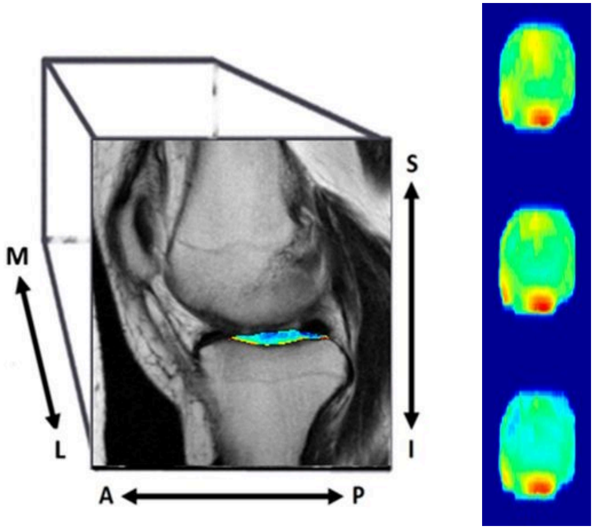

TBM in early detection of osteoarthritis (OA)

Images acquired 3 years prior to symptoms

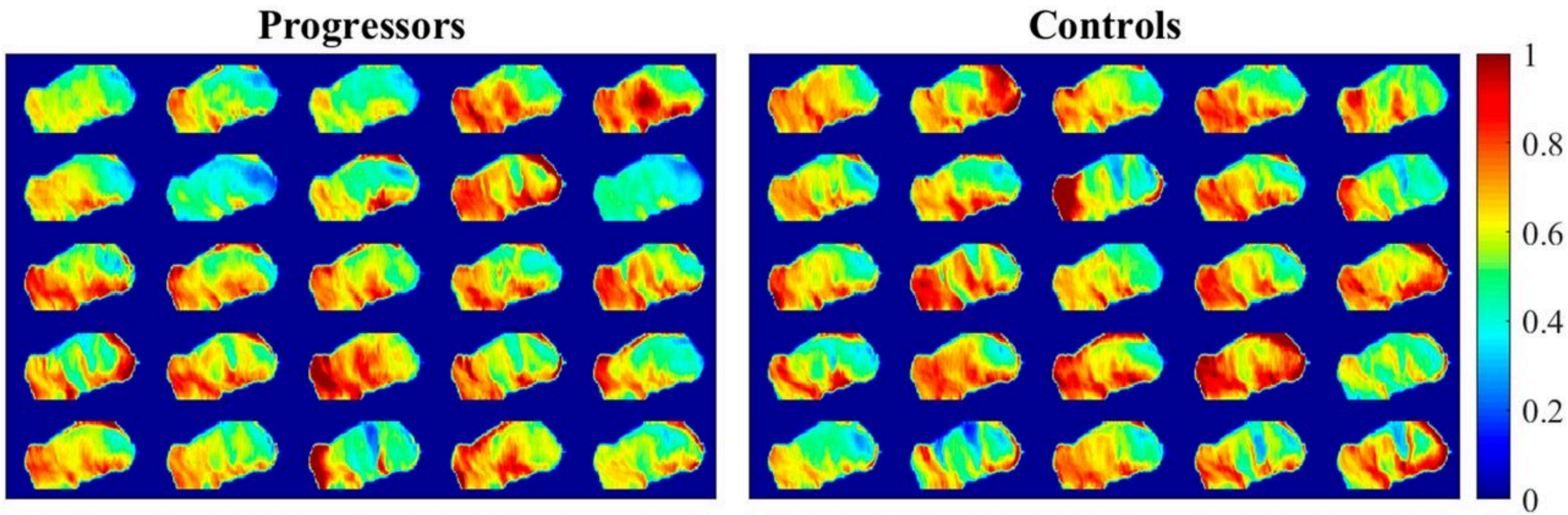

Can we predict which ones will progress to be symptomatic 3 years in the future?

(ground truth diagnosis based on WOMAC score, 86 subjects)

Presymptomatic prediction accuracy

Classifier for cartilage texture maps	Test accuracy, %	Sensitivity, %	Specificity, %	Cohen's kappa	*P*
Original image pLDA	64.5	61.5	67.4	0.29	< 0.001
Original image SVM (Gaussian kernel)	63.2	65.5	60.9	0.26	<0.001
Original image RF	54.9	39.0	70.7	0.10	<0.001
TBM pLDA	78.0	76.9	79.0	0.56	<0.001
TBM SVM (Gaussian kernel)	74.1	78.0	70.2	0.48	<0.001
TBM RF	70.2	65.0	75.3	0.40	<0.001
WNDCHRM features pLDA	60.8	60.6	61.0	0.22	0.02
WNDCHRM features SVM (Gaussian kernel)	53.3	62.7	43.9	0.07	0.19
WNDCHRM features RF	55.6	48.6	62.6	0.11	<0.001

Classifier inverse:

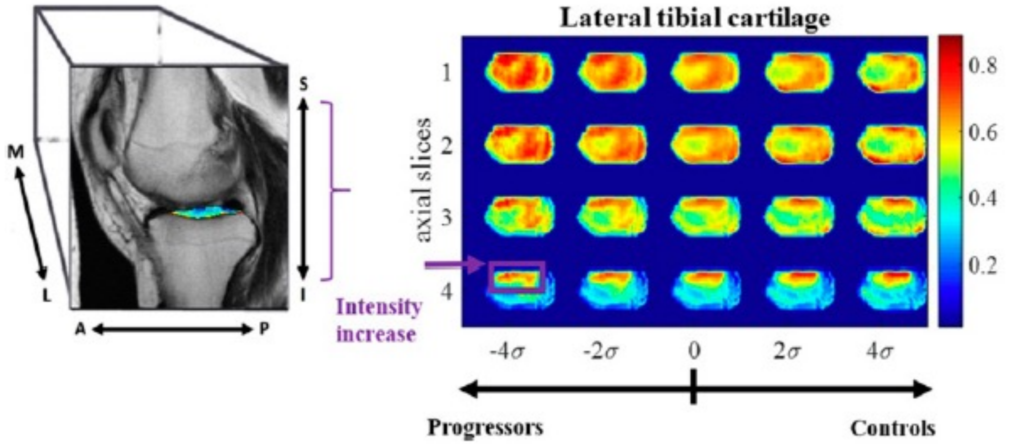

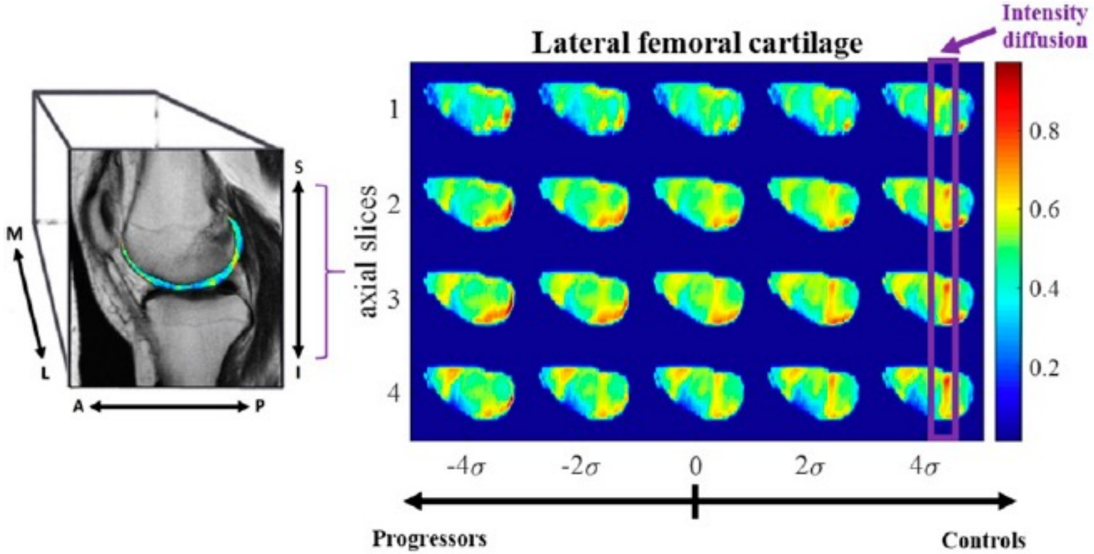

[Kundu, Ashinsky, Bouhrara, Dam, Demehri, Shifat-E-Rabbi, Spencer, Urish, Rohde, PNAS, 2020]

Summary: transport-based morphometry

1) Exploratory analysis

- Transport PCA, subspace learning, …
- Models texture & shape simultaneously
- Visualizes variations within dataset

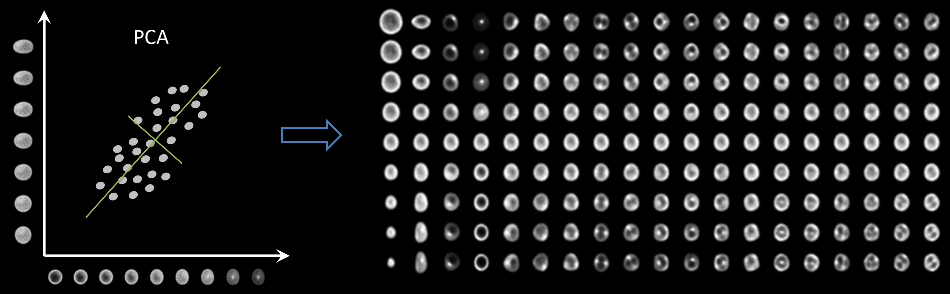

2) Discriminant models

- SVM, LDA, pLDA, …
- Visualizes most discriminative information

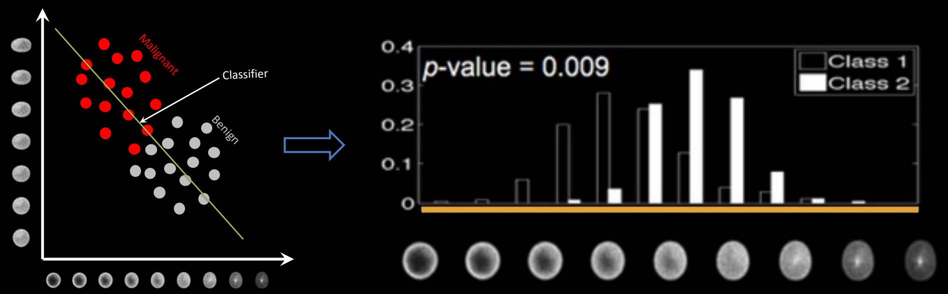

3) Functional relationships

- CCA
- Study & visualize relationship between different measurements

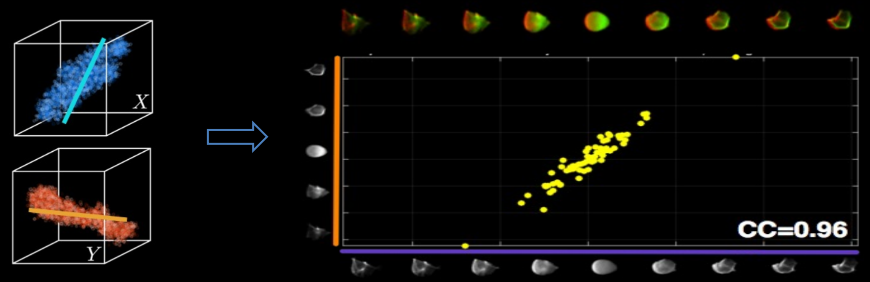

Signa/image classification

Agebraic generative model for signal/image classes

An image class is modeled as

a set of transport maps $g_j \in \mathcal{G}$

applied to a template $\varphi^{(k)}$

unknown

$\mathbb{S}^1$: class for digit 1

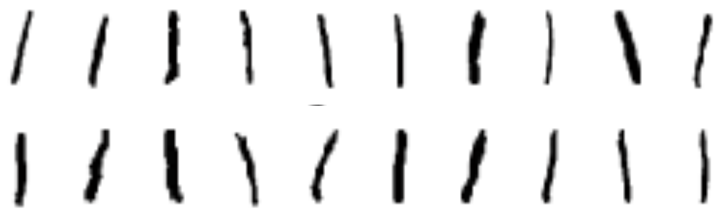

$$\mathbb{S}^{(1)} = \left\{ s_j^{(1)} | s_j^{(1)} = |\det J g_j| \varphi^{(1)} \circ g_j, \forall g_j \in \mathcal{G} \right\}$$

template for class 1 $\varphi^{(1)} =$

"confound"

$\mathbb{S}^2$: class for digit 2

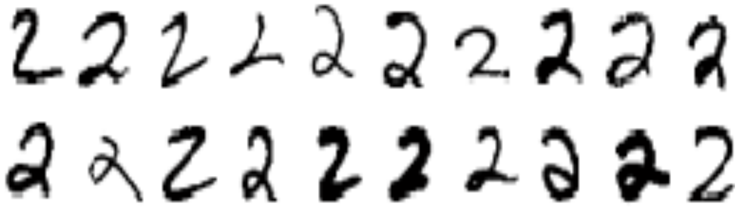

$$\mathbb{S}^{(2)} = \left\{ s_j^{(2)} | s_j^{(2)} = |\det J g_j| \varphi^{(2)} \circ g_j, \forall g_j \in \mathcal{G} \right\}$$

template for class 2 $\varphi^{(2)} =$ 

Model for 1D signal classes

$\mathbb{S}^{(1)}$: class for normal ECG heartbeats

$$\mathbb{S}^{(1)} = \{\boldsymbol{s}_j^{(1)} | \boldsymbol{s}_j^{(1)} = \boldsymbol{g}'_j \varphi^{(1)} \circ \boldsymbol{g}_j, \forall \boldsymbol{g}_j \in \mathcal{G}\}$$

template for class 1: $\varphi^{(1)}$

$\mathbb{S}^{(2)}$: class for premature ventricular contraction beats

$$\mathbb{S}^{(2)} = \{\boldsymbol{s}_j^{(2)} | \boldsymbol{s}_j^{(2)} = \boldsymbol{g}'_j \varphi^{(2)} \circ \boldsymbol{g}_j, \forall \boldsymbol{g}_j \in \mathcal{G}\}$$

template for class 2: $\varphi^{(2)}$

Problem statement (supervised learning)

Training: given sample signals/images from different classes

$$\{s_1^{(1)}, s_2^{(1)}, \cdots\} \qquad s_j^{(k)} \in \mathbb{S}^{(k)} = \left\{ s_j^{(k)} | s_j^{(k)} = |\det J g_j| \varphi^{(k)} \circ g_j, \forall g_j \in \mathcal{G} \right\}$$

$$\{s_1^{(2)}, s_2^{(2)}, \cdots\}$$

$\varphi^{(k)}$ unknown

$g_j \in \mathcal{G}$ unknown

Testing: find the class that a test sample s originated from.

Solution overview

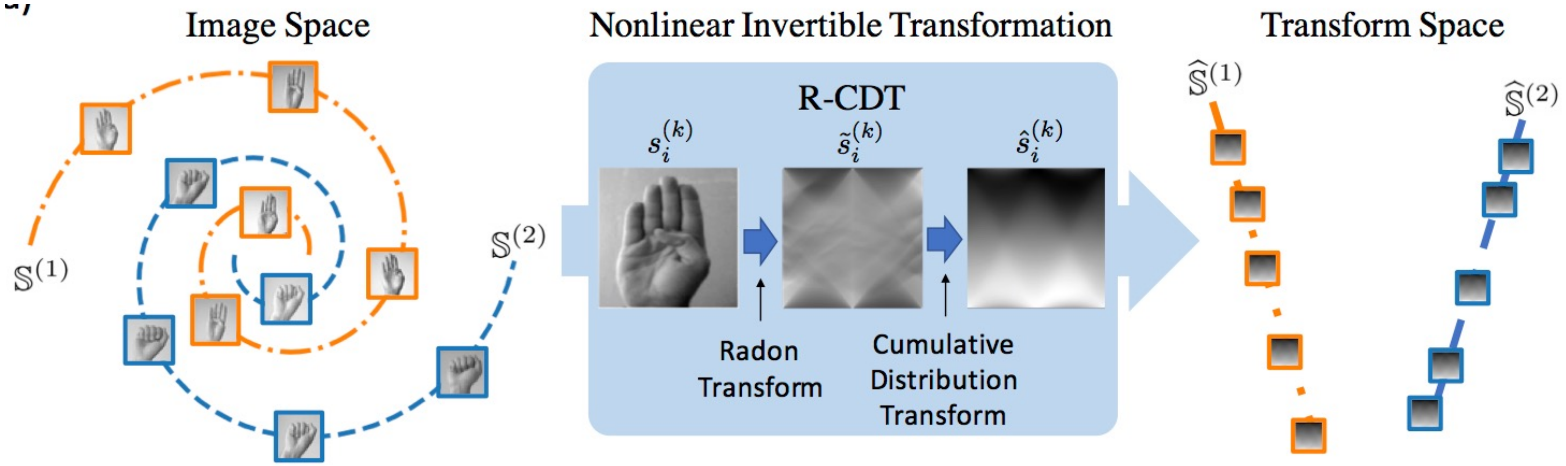

RCDT – nearest subspace

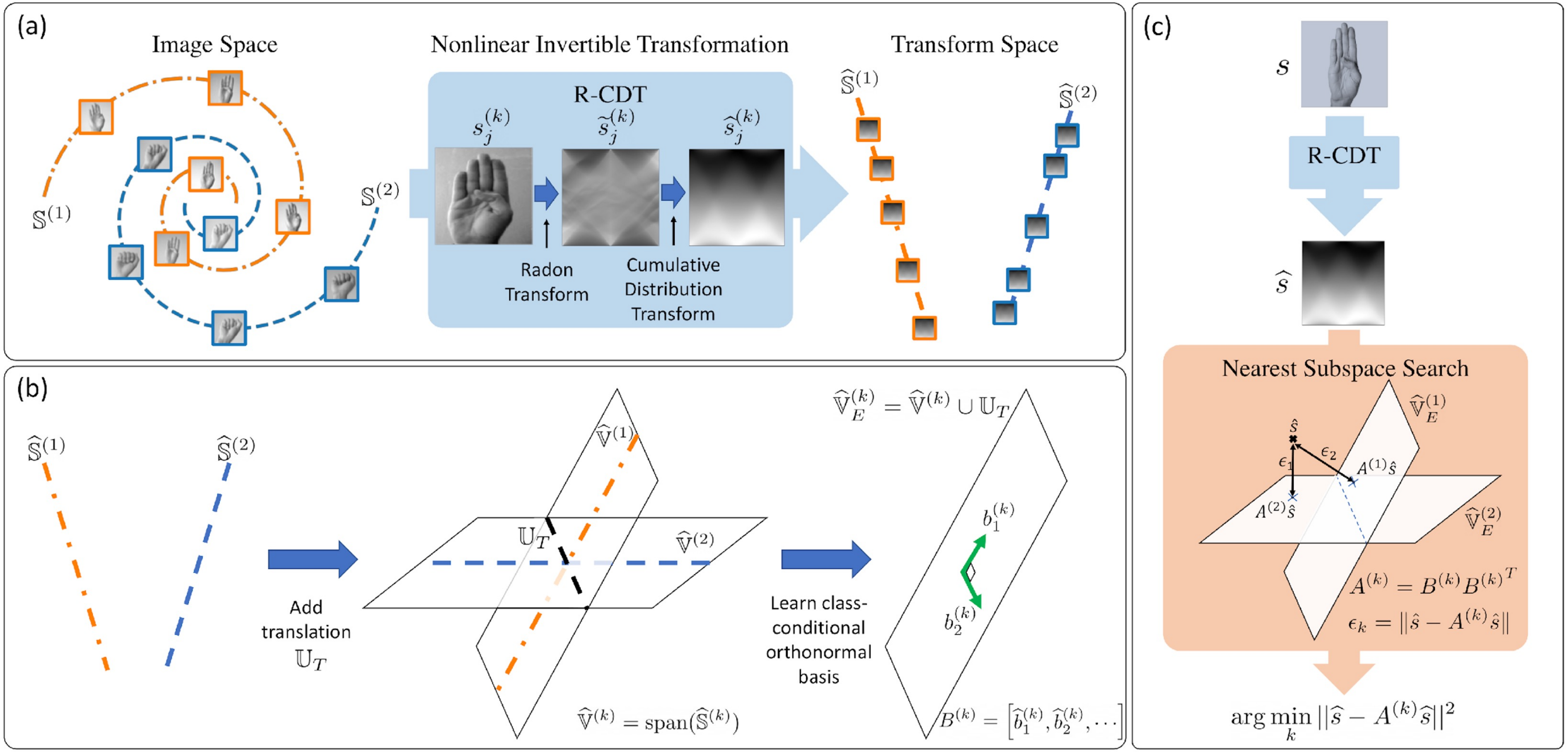

RCDT – nearest subspace

Training: estimating basis vectors for subspaces corresponding to each class

training data $\left\{s_1^{(k)}, s_2^{(k)}, \cdots\right\}$ → transform $\left\{\widehat{s}_1^{(k)}, \widehat{s}_2^{(k)}, \cdots\right\}$ → deformation model $\left\{\widehat{s}_1^{(k)}, \widehat{s}_2^{(k)}, \cdots\right\} \cup \mathbb{U}_T$ → orthogonalize $\left[\widehat{b}_1^{(k)}, \widehat{b}_2^{(k)}, \cdots\right] = B^{(k)}$ → output $B^{(k)}$

Testing : predicting the test sample as belonging to the class corresponding to the nearest subspace

test sample s → transform $\hat{s}$ → nearest subspace $\arg\min_k ||\widehat{s} - A^{(k)}\widehat{s}||^2$ → class 1, class 2, ⋮

Here, $A^{(k)} = B^{(k)} {B^{(k)}}^T$

Translation $\mathbb{U}_T = \{u_T^{(1)}(t,\theta), u_T^{(2)}(t,\theta)\}$, with $u_T^{(1)}(t,\theta) = \cos\theta$ and $u_T^{(2)}(t,\theta) = \sin\theta$

Isotropic scaling $\mathbb{U}_D = \varnothing$

Two important aspects of the method:

1. The method can learn from datasets
2. The method can learn from mathematically prescribed sets without explicitly using the training data

Datasets

Chinese printed character dataset

MNIST dataset

Affine-MNIST dataset

Optical OAM dataset

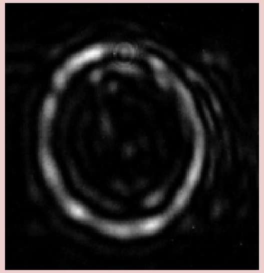

Sign language dataset

OASIS Brain MRI dataset

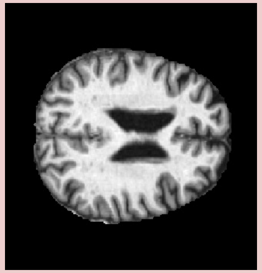

Results and comparisons with deep learning

[Shifat-E-Rabbi et al, JMIV 2021]

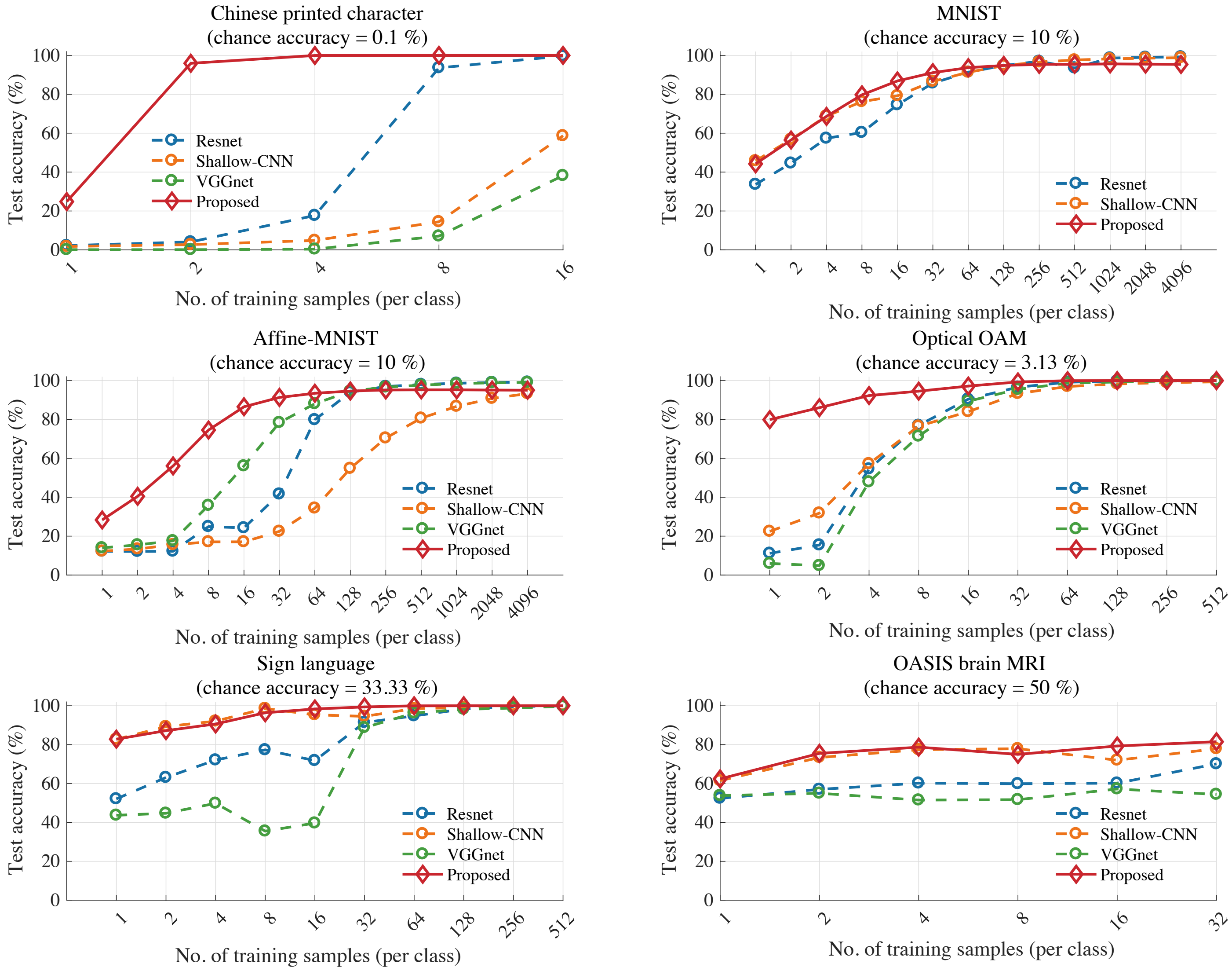

Out of distribution testing

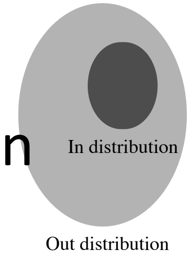

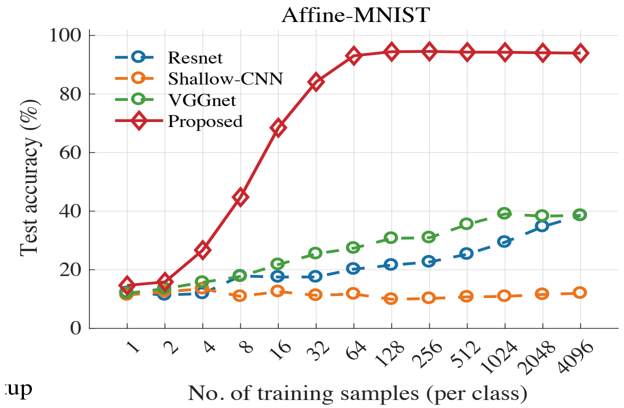

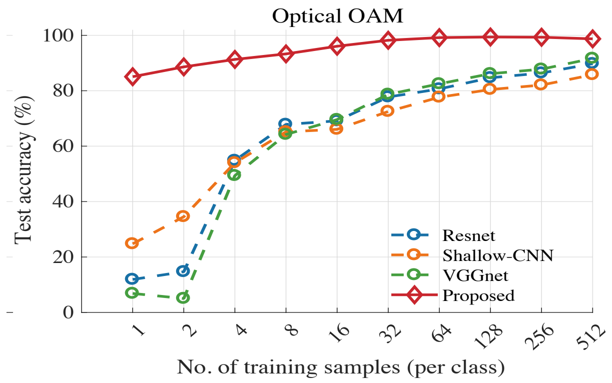

Results and comparisons with deep learning

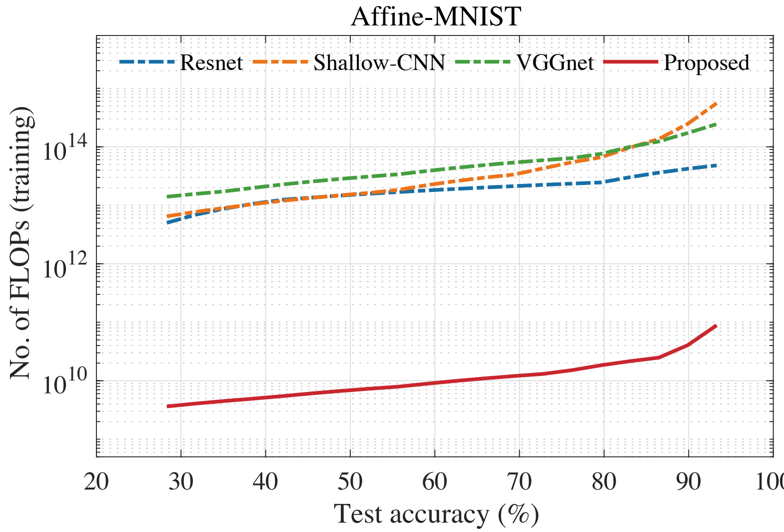

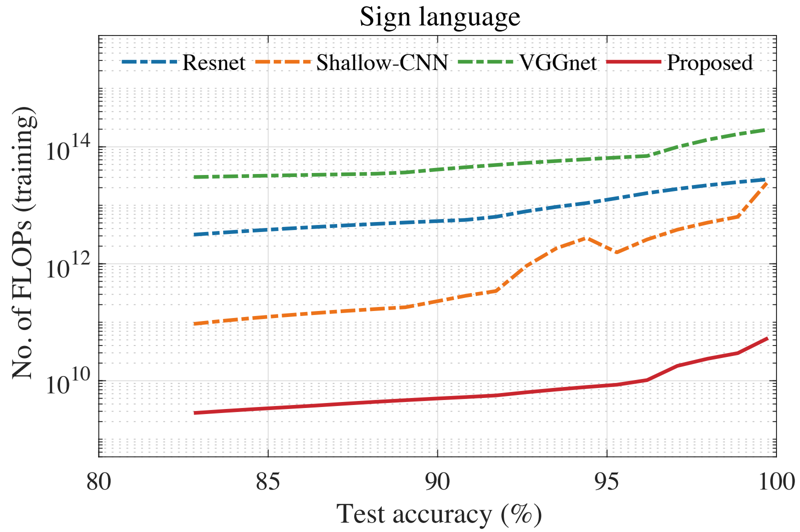

Limitations

$$\mathbb{P} = \{p_g : g \in \mathcal{C}\} \quad \mathbb{Q} = \{q_g : g \in \mathcal{C}\}$$

where

$$p_g(x) = g'(x)p_0(g(x))$$
$$q_g(x) = g'(x)q_0(g(x))$$

It doesn't seem to work as well for general object detection

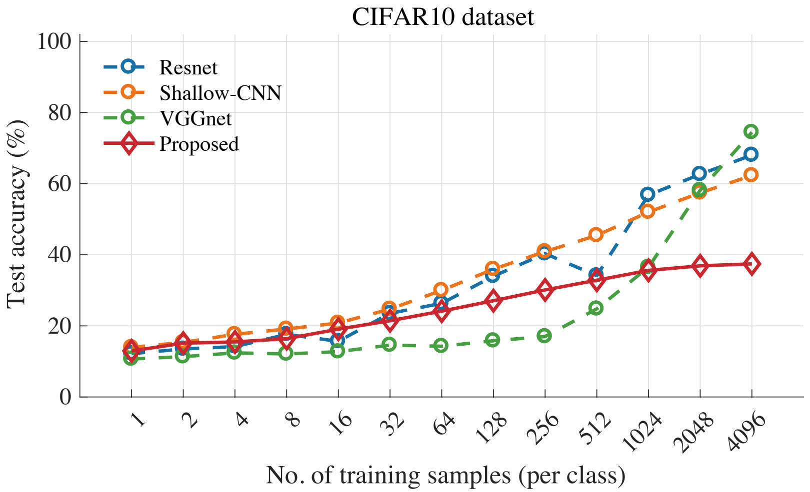

Invariance encoding

Aim: Can we mathematically model invariances ?

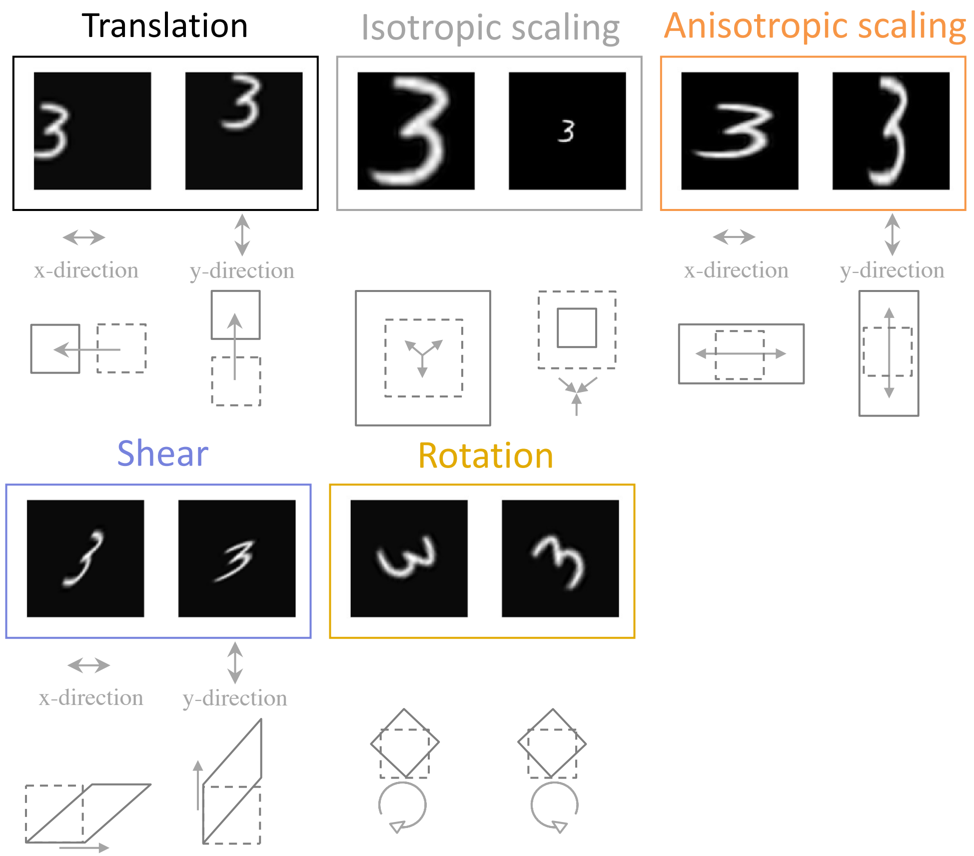

$$\{s_1^{(1)}, s_2^{(1)}, \cdots\} \quad \{s_1^{(2)}, s_2^{(2)}, \cdots\}$$

$$s_j^{(k)} \in \mathbb{S}^{(k)} = \left\{ s_j^{(k)} | s_j^{(k)} = |\det J g_j| \varphi^{(k)} \circ g_j, \forall g_j \in \mathcal{G} \right\}$$

$\varphi^{(k)}$ unknown $\quad g_j \in \mathcal{G}$ unknown + affine

Solution overview:

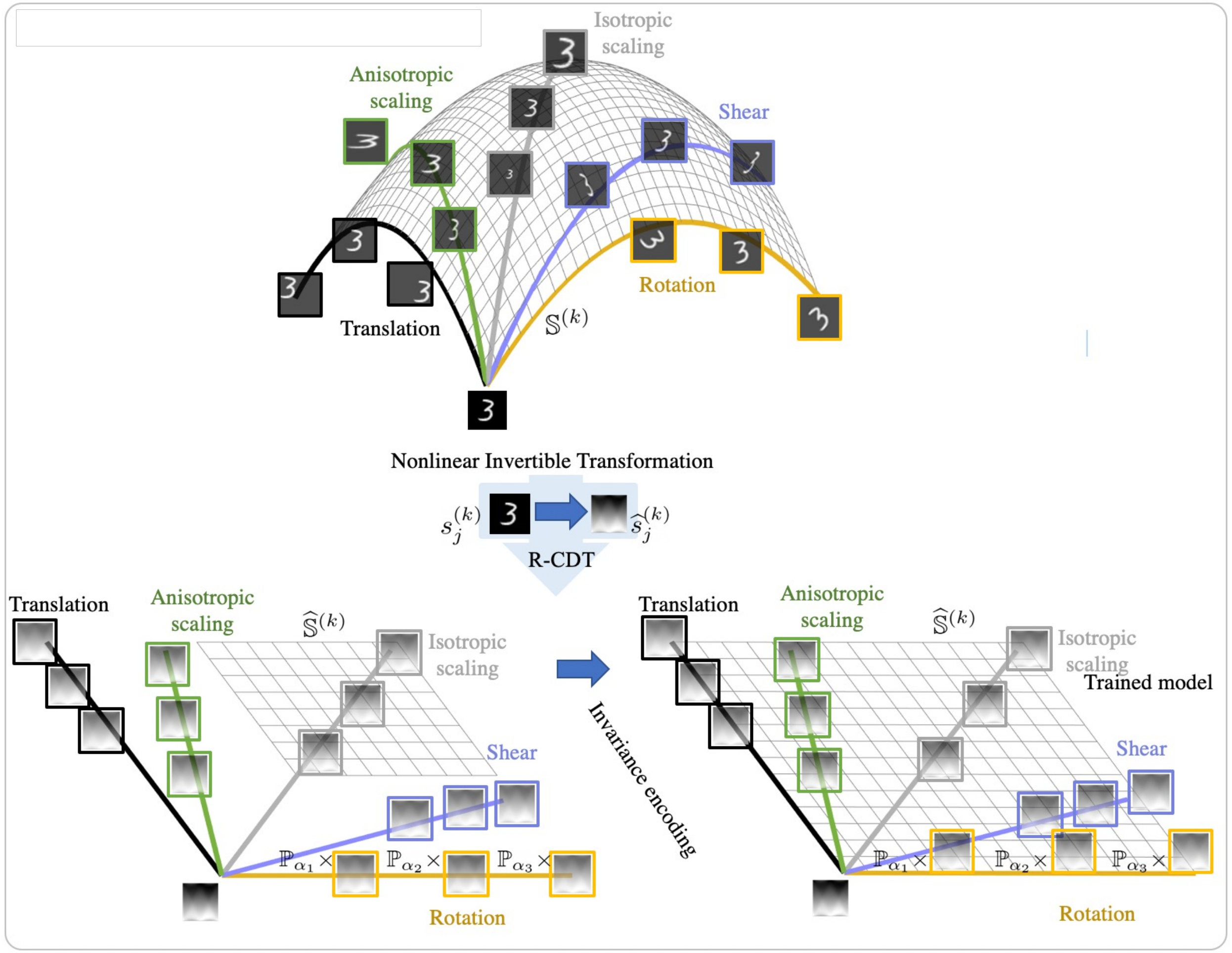

Results and comparisons with deep learning

[Shifat-E-Rabbi et al, arxiv 2022]

Synthetic data

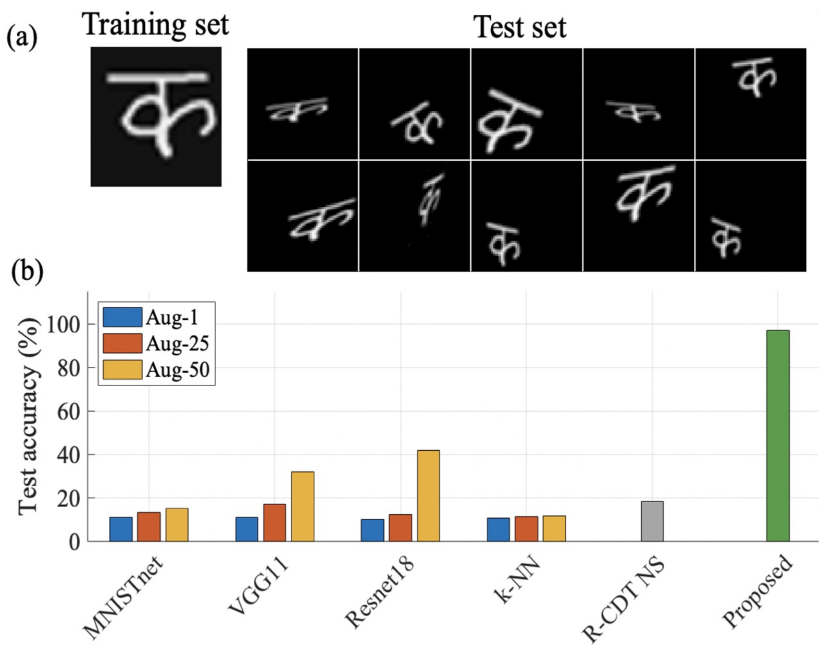

Real data

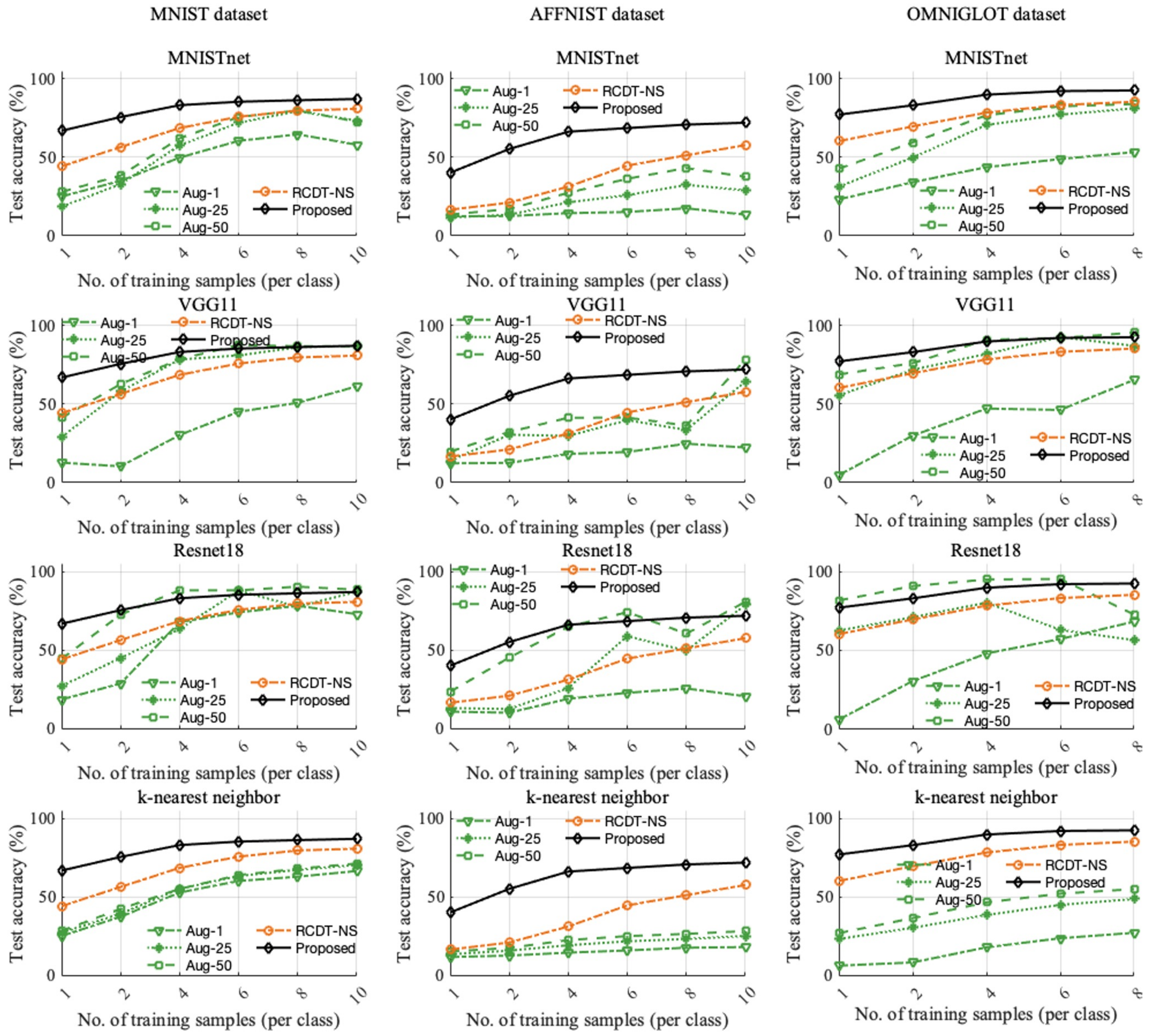

Results and comparisons with deep learning

[Shifat-E-Rabbi et al, arxiv 2022]

Computational complexity

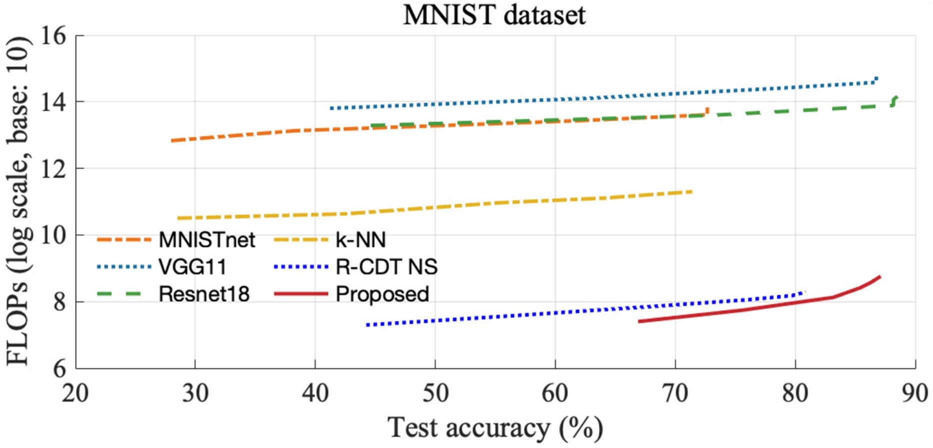

Out-of-distribution experiment

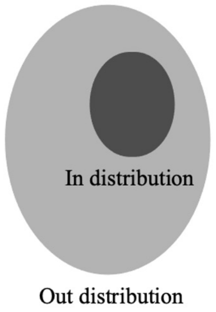

Out of distribution setup

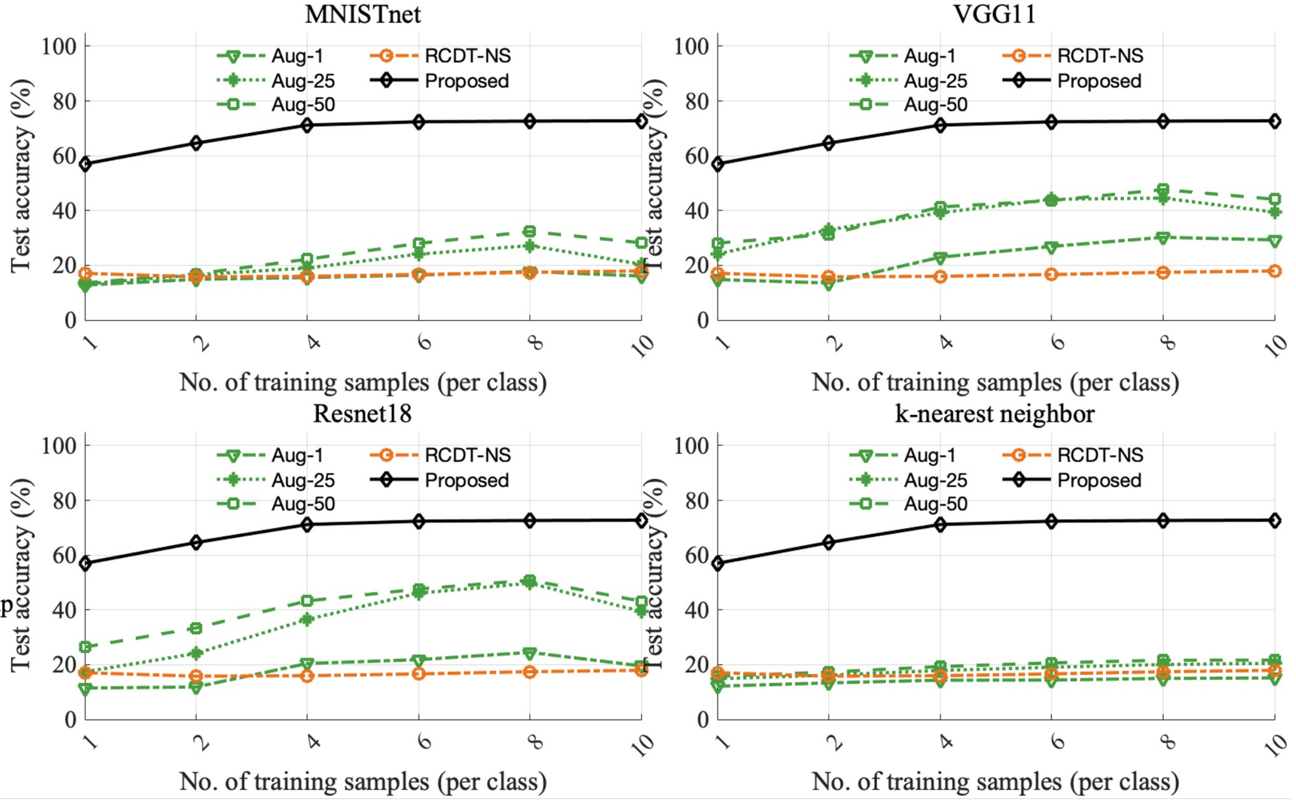

End-to-End Time Series Classification [Rubaiyat et al, ArXiv 2022]

Generative Model:

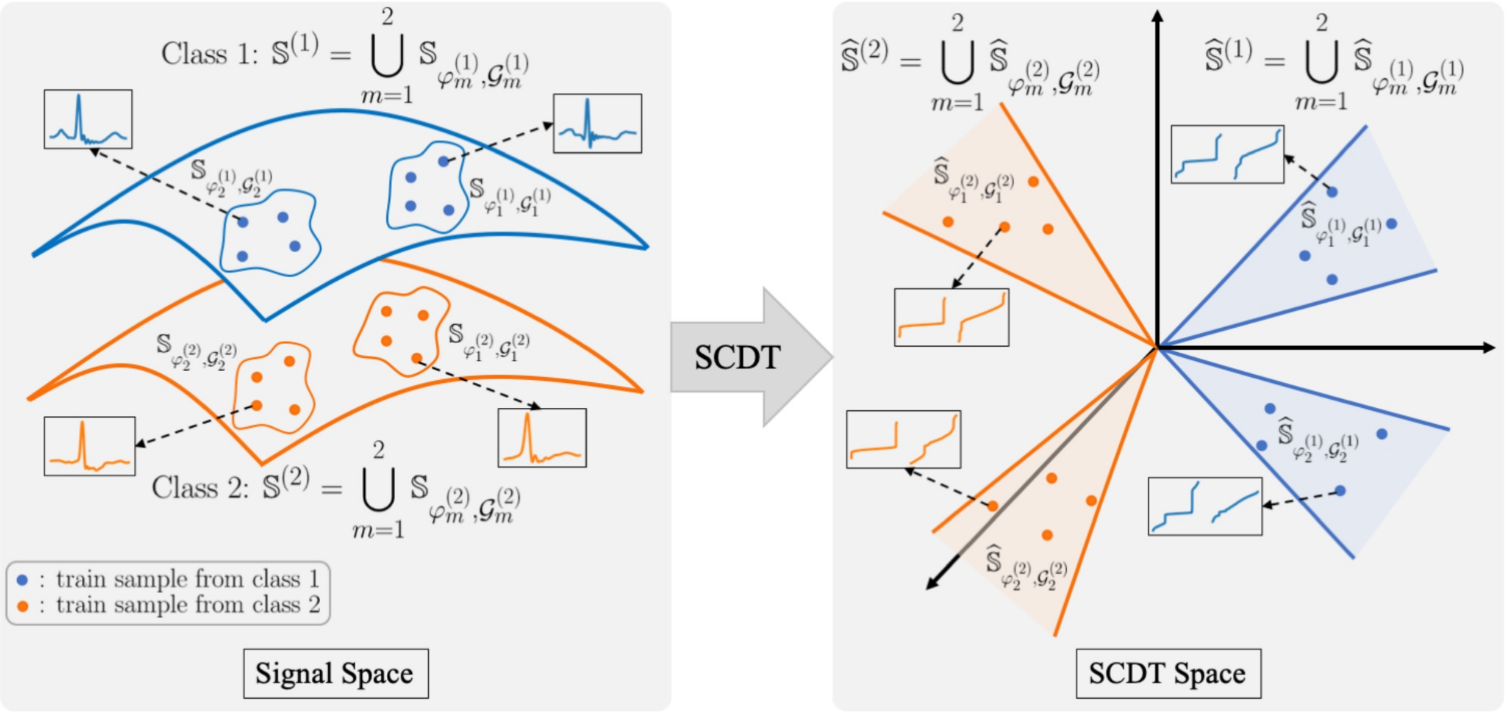

$$\mathbb{S}^{(c)} = \bigcup_{m=1}^{M_c} \mathbb{S}_{\varphi_m^{(c)},\mathcal{G}_m^{(c)}},$$

$$\mathbb{S}_{\varphi_m^{(c)},\mathcal{G}_m^{(c)}} = \left\{ s_{j,m}^{(c)} \middle| s_{j,m}^{(c)} = g_j' \varphi_m^{(c)} \circ g_j, g_j' > 0, g_j \in \mathcal{G}_m^{(c)} \right\},$$

$$\left(\mathcal{G}_m^{(c)}\right)^{-1} = \left\{ \sum_{i=1}^{k} \alpha_i f_{i,m}^{(c)}, \alpha_i \geq 0 \right\}$$

$$\widehat{\mathbb{S}}^{(c)} = \bigcup_{m=1}^{M_c} \widehat{\mathbb{S}}_{\varphi_m^{(c)},\mathcal{G}_m^{(c)}},$$

$$\widehat{\mathbb{S}}_{\varphi_m^{(c)},\mathcal{G}_m^{(c)}} = \left\{ \widehat{s}_{j,m}^{(c)} \middle| \widehat{s}_{j,m}^{(c)} = g_j^{-1} \circ \widehat{\varphi}_m^{(c)}, g_j \in \mathcal{G}_m^{(c)} \right\},$$

$$\left(\mathcal{G}_m^{(c)}\right)^{-1} = \left\{ \sum_{i=1}^{k} \alpha_i f_{i,m}^{(c)}, \alpha_i \geq 0 \right\}$$

End-to-End Time Series Classification [Rubaiyat et al, ArXiv 2022]

NLS algorithm:

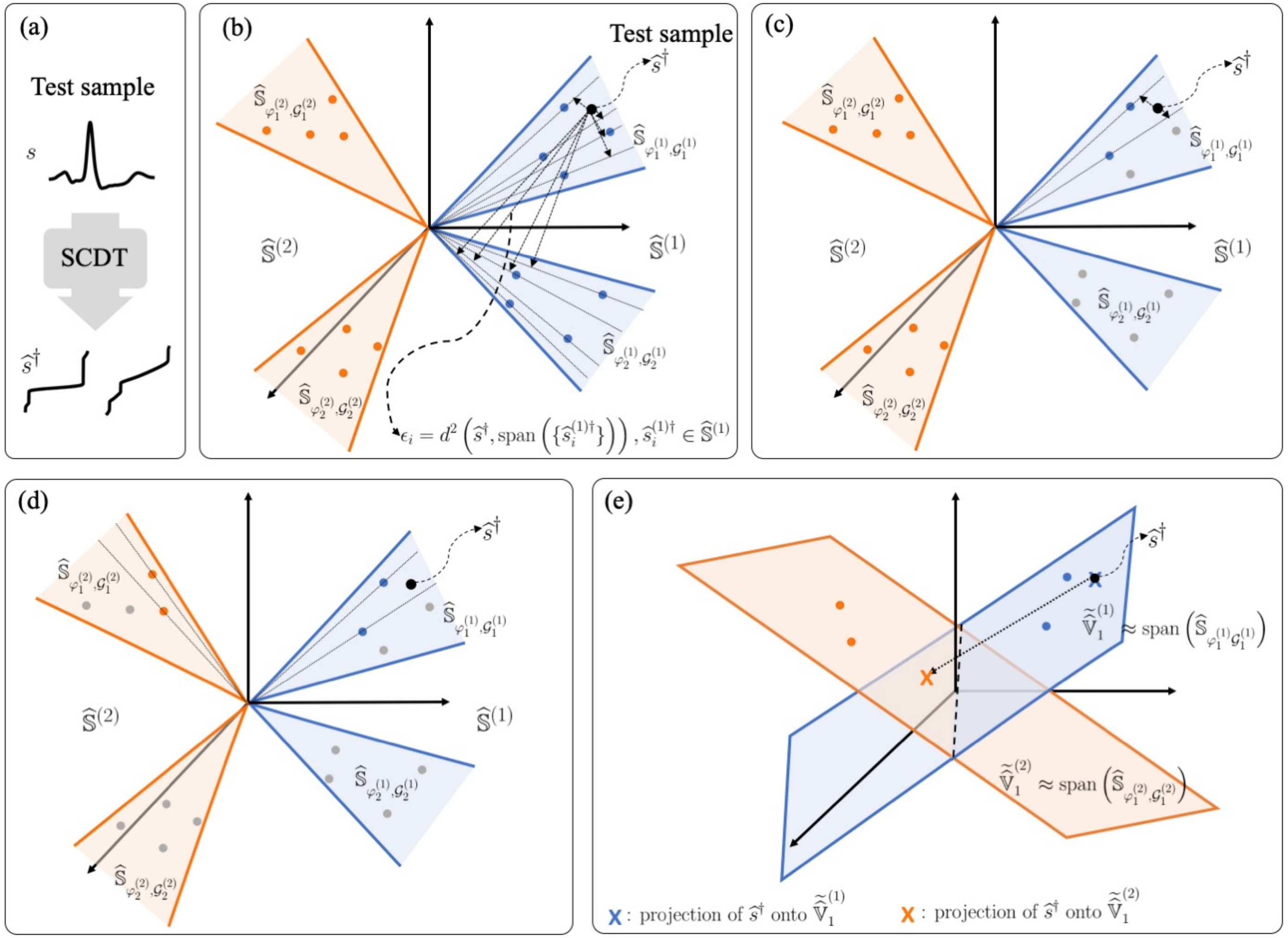

Subspace Enrichment:

$$\widetilde{\widehat{\mathbb{V}}}^{(c)}_m = \text{span}\left(\{\widehat{z}_1^{(c)\dagger}, \cdots, \widehat{z}_k^{(c)\dagger}\} \cup \mathbb{U}_T \cup \mathbb{U}_H\right)$$

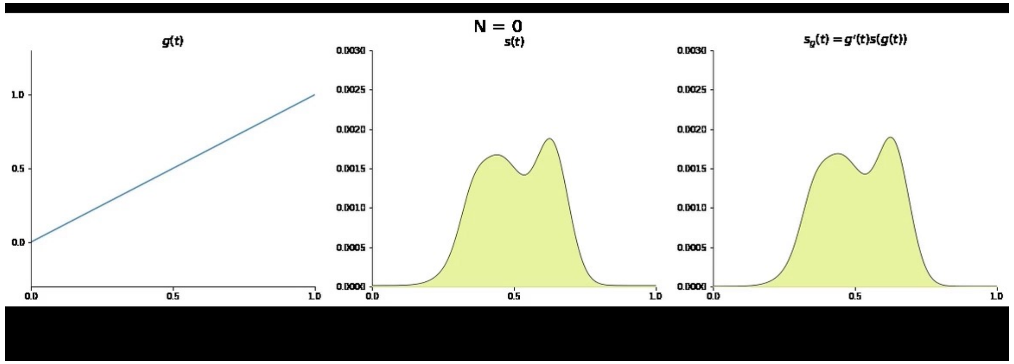

Solution is given by: $\underset{c}{\arg\min}\ d^2\left(\widehat{s}, \widetilde{\widehat{\mathbb{V}}}^{(c)}_m\right)$

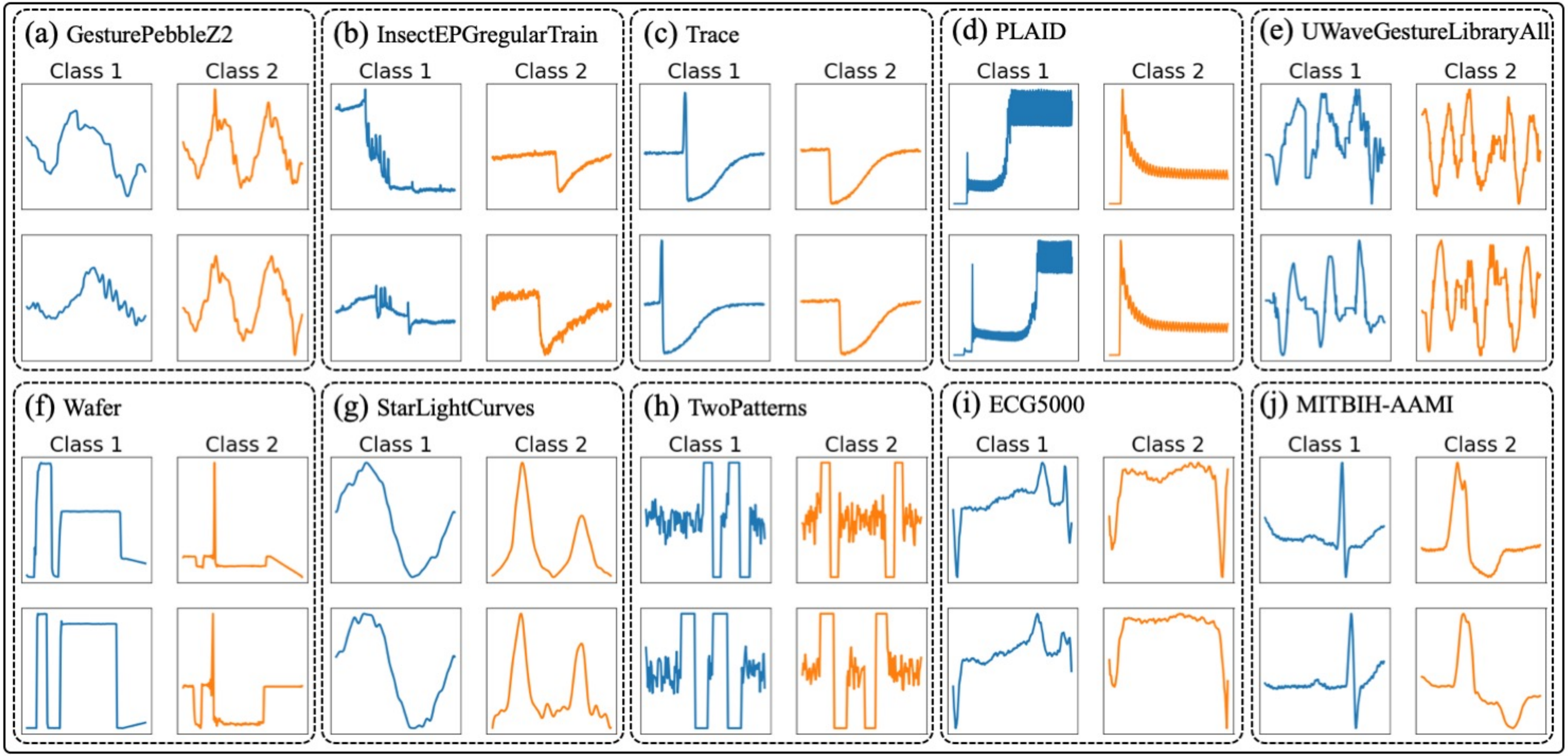
(a) GesturePebbleZ2
Class 1
Class 2
(b) InsectEPGregularTrain
Class 1
Class 2
(c) Trace
Class 1
Class 2
(d) PLAID
Class 1
Class 2
(e) UWaveGestureLibraryAll
Class 1
Class 2
(f) Wafer
Class 1
Class 2
(g) StarLightCurves
Class 1
Class 2
(h) TwoPatterns
Class 1
Class 2
(i) ECG5000
Class 1
Class 2
(j) MITBIH-AAMI
Class 1
Class 2

Results and comparisons with deep learning

[Rubaiyat et al, ArXiv 2022]

Dataset	MLP	1D-VGG	1D-ResNet	LSTM	LSTM-FCN	SCDT-NS	**Proposed**
GesturePebbleZ2	83.92	48.99	63.23	60.19	85.82	81.64	**86.07**
InsectEPGRegularTrain	80.92	82.07	50.58	57.05	59.95	73.43	**90.82**
Trace	64.0	35.8	25.9	28.2	58.1	85.0	**88.0**
PLAID	39.65	19.35	29.81	26.35	39.57	58.29	**70.02**
UWaveGestureLibraryAll	94.74	**96.42**	42.86	30.72	94.16	90.4	94.92
Wafer	68.69	94.03	53.66	51.36	86.70	92.75	**95.53**
StarLightCurves	75.85	70.0	56.53	60.54	74.38	77.4	**84.2**
TwoPatterns	88.12	95.15	87.42	80.62	98.47	95.15	**99.92**
ECG5000	98.9	**98.92**	**98.92**	98.36	98.76	93.4	97.4
MITBIH-AAMI	65.54	82.94	59.13	55.34	79.46	62.9	**84.05**
Win	0	2	1	0	0	0	**8**
AVG arithmetic ranking	3.5	3.5	5.6	6.3	3.6	3.8	**1.6**
AVG geometric ranking	3.42	2.8	5.07	6.27	3.46	3.49	**1.28**
MPCE	0.072	0.065	0.125	0.127	0.066	0.059	**0.030**

Out of distribution testing

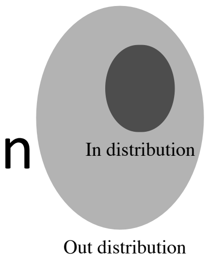

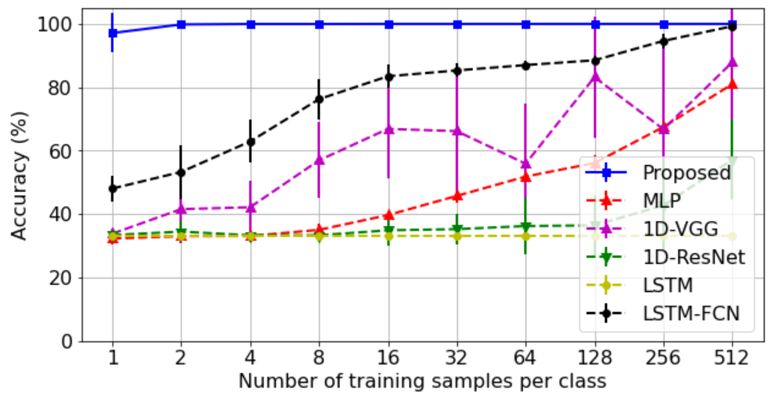

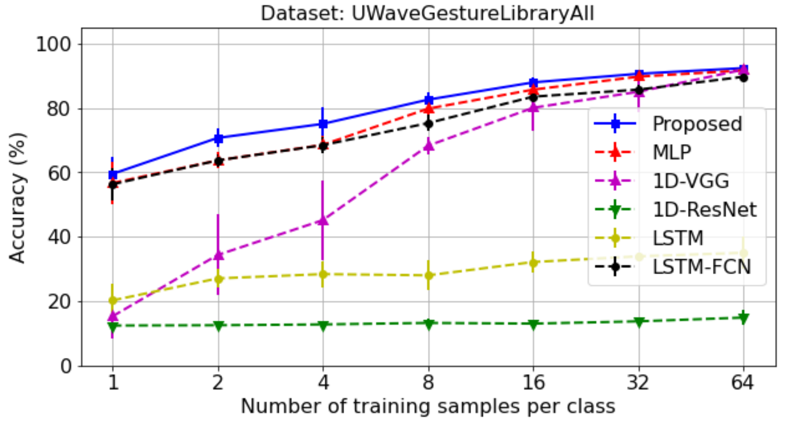

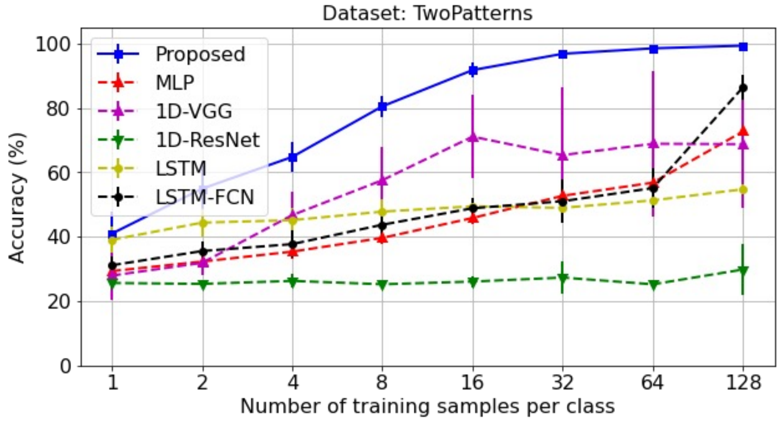

Other applications

Kolouri et al, *Wasserstein Embedding for Graph Learning*, ICLR 2021

Uses LOT to obtain embedding for graph features for classification

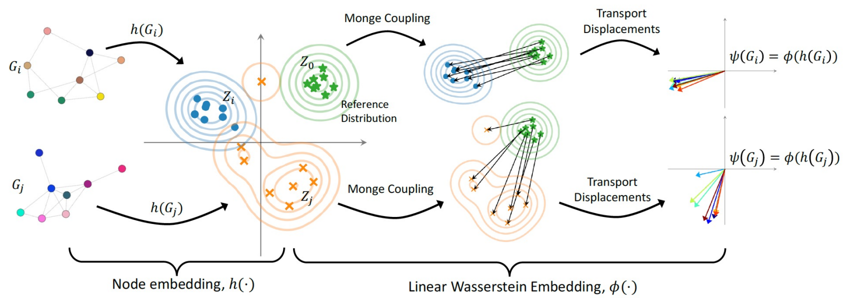

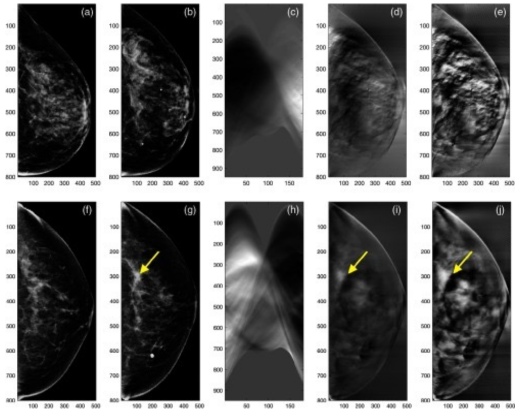

Lee et al, *Detecting mammographically occult cancer in women with dense breasts using deep convolutional neural network and Radon Cumulative Distribution Transform*, Journal of Medical Imaging 2019.

Cai et al, *Linearized optimal transport for collider events*. Physical Review D, 2020.

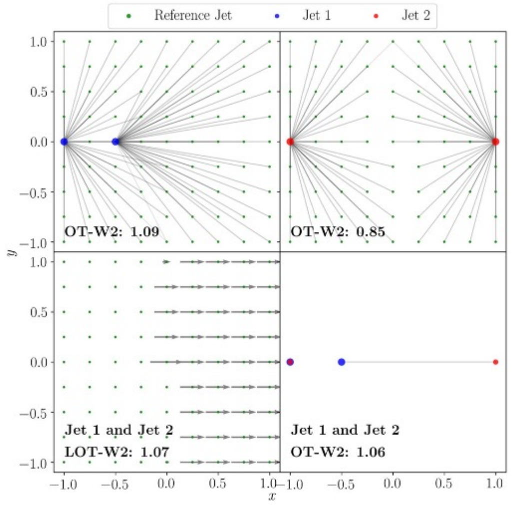

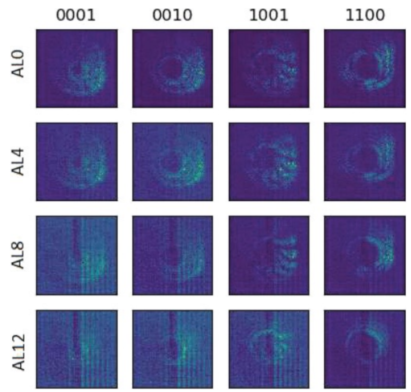

Neary et al, *Tranposrt-based pattern recognition versus deep neural networks in underwater OAM communications,* JOSA (A), 2021.

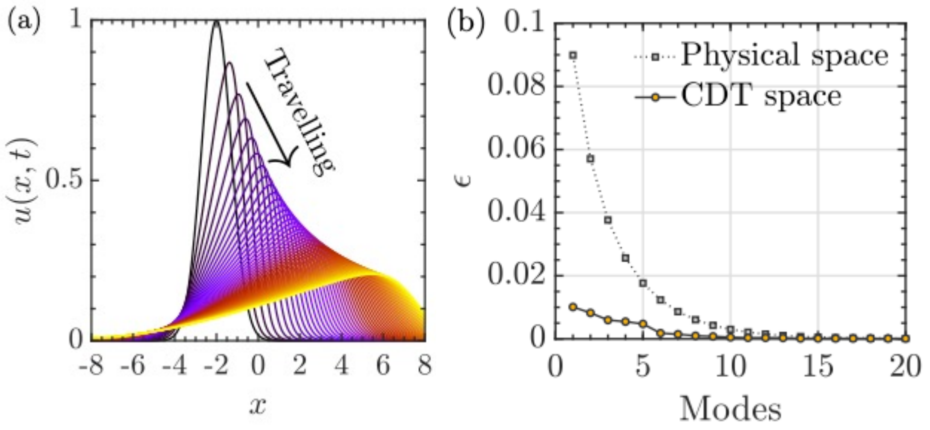

Ren et al, *Model reduction of traveling-wave problems via Radon cumulative distribution transform,* Physical Review Fluids, 2021.

Zhuang et al, *Local sliced-Wasserstein features sets for illumination-invariant face recognition, ArXiv, 2022*.

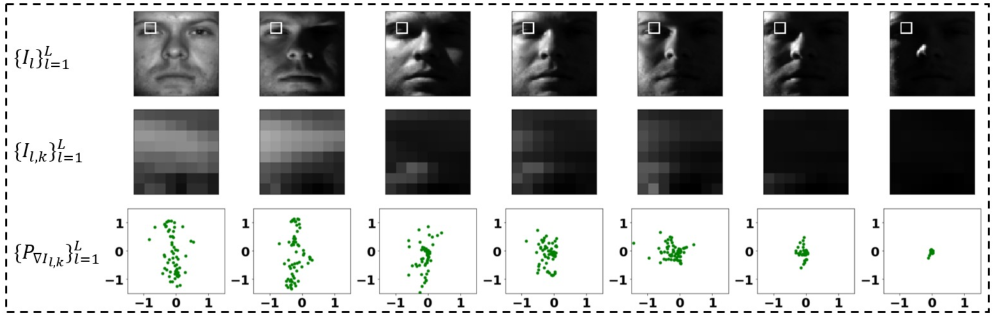

Summary

nonlinear system

$$s \Rightarrow \boxed{\begin{array}{c} g' s \circ g \\ g = \nabla \phi \end{array}} \Rightarrow \tilde{s}$$

least action
conservative

Solution

signal space		transform space		signal space
problem hard to solve	$\Rightarrow$	problem easy to solve	$\Rightarrow$	answer in signal space

estimation, detection,
inverse problems, classification

Extra slides

Post-concussive cognitive changes

- Immediate and transient alteration in brain function
- Cognitive changes are common after mild traumatic brain injury and predictive of poor post-concussive outcome (Himanen et al. 2005; Bigler, 2004)
- However, the underlying **structural substrates** are poorly understood
- Diffuse axonal injury implicated in decrease in working memory (Niogi et al. 2008)

Kundu, Ghodadra, Fakhran, Alhilali, Rohde, Assessing Post-concussive reaction time using TBM of diffusion tensor images, American Journal of Neuroradiology, 2019.

Goals

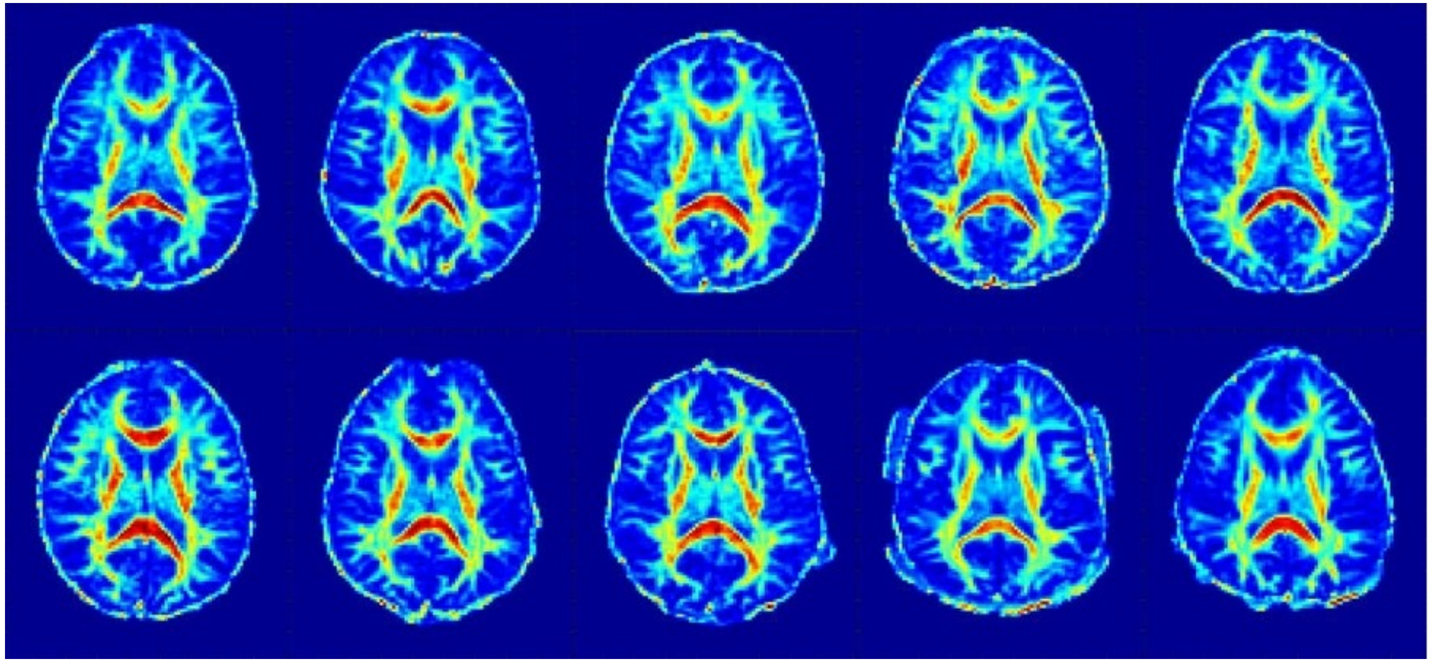

- **Are there identifiable patterns that are hidden from human view?**
- **If so, how can we find them?**

Visualization of dynamic morphology changes

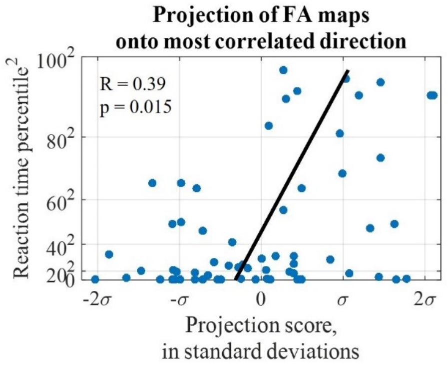

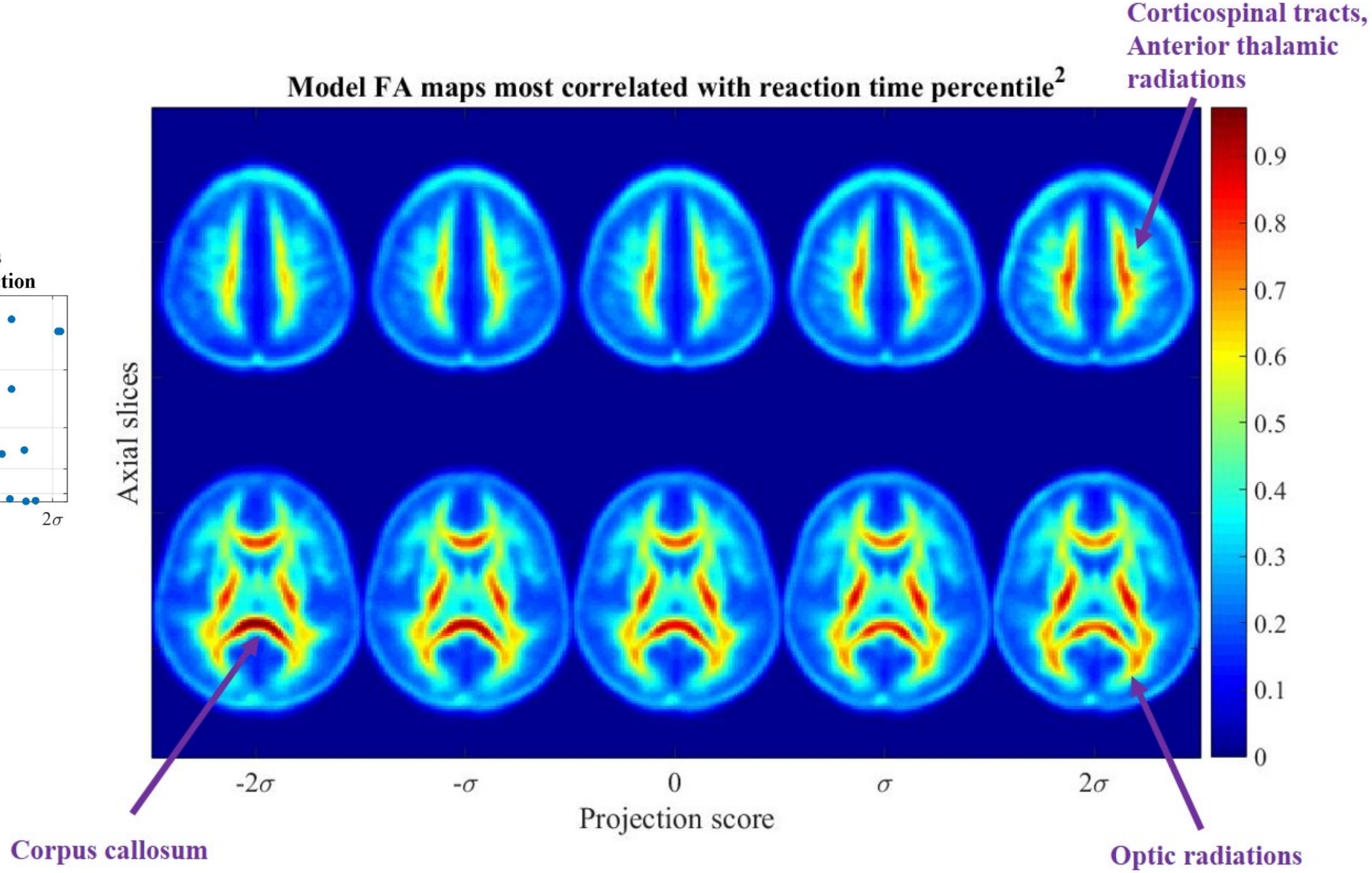

Kundu, Ghodadra, Fakhran, Alhilali, Rohde, Assessing Post-concussive reaction time using TBM of diffusion tensor images, American Journal of Neuroradiology, 2019.

T1 images and aging

White matter with age

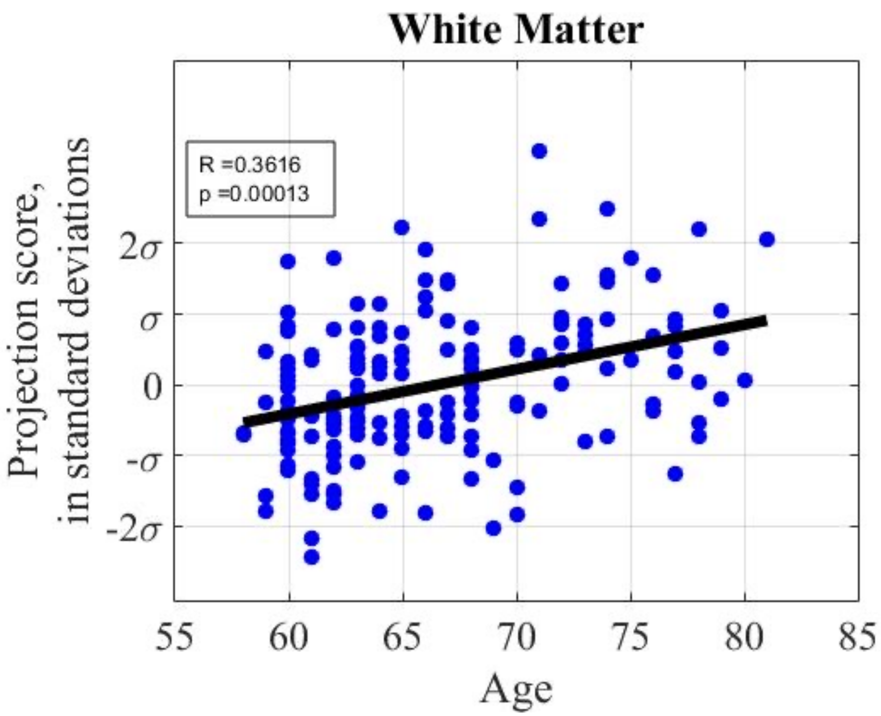

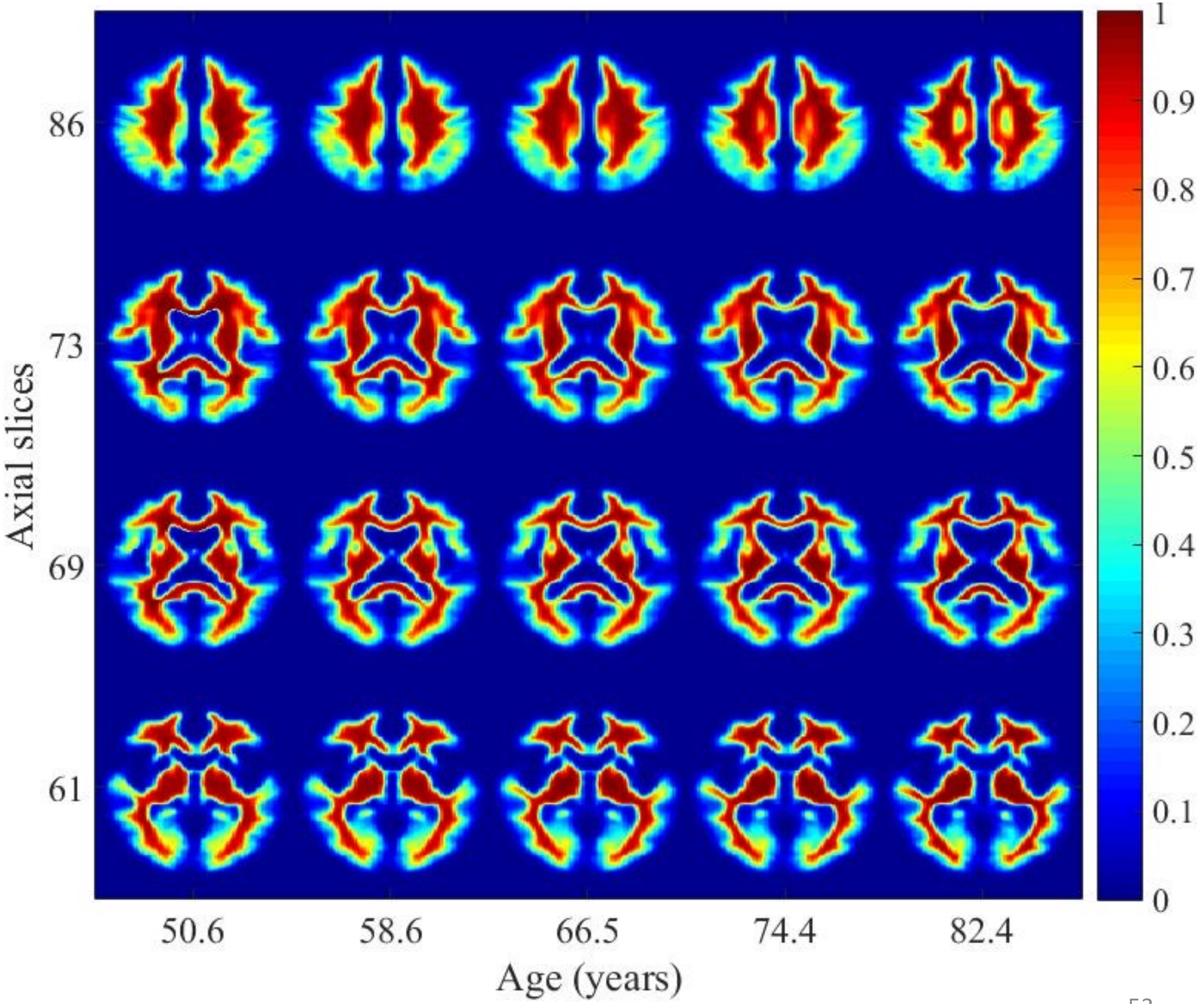

0.31 mm shift in GM distribution with every 10 year increase age.

Gray matter with age

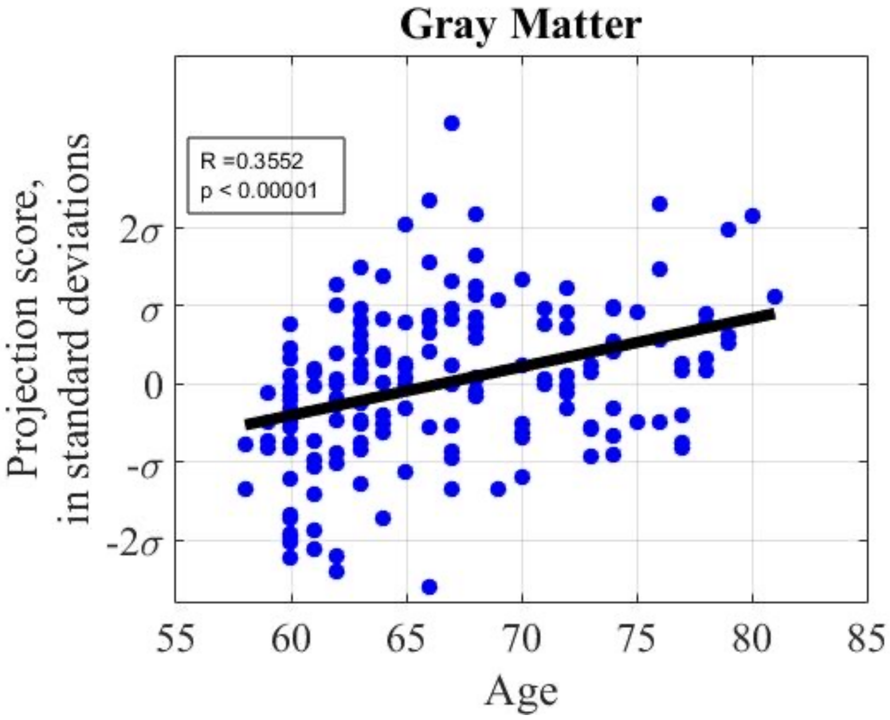

0.66 mm shift in GM distribution with every 10 year increase age.

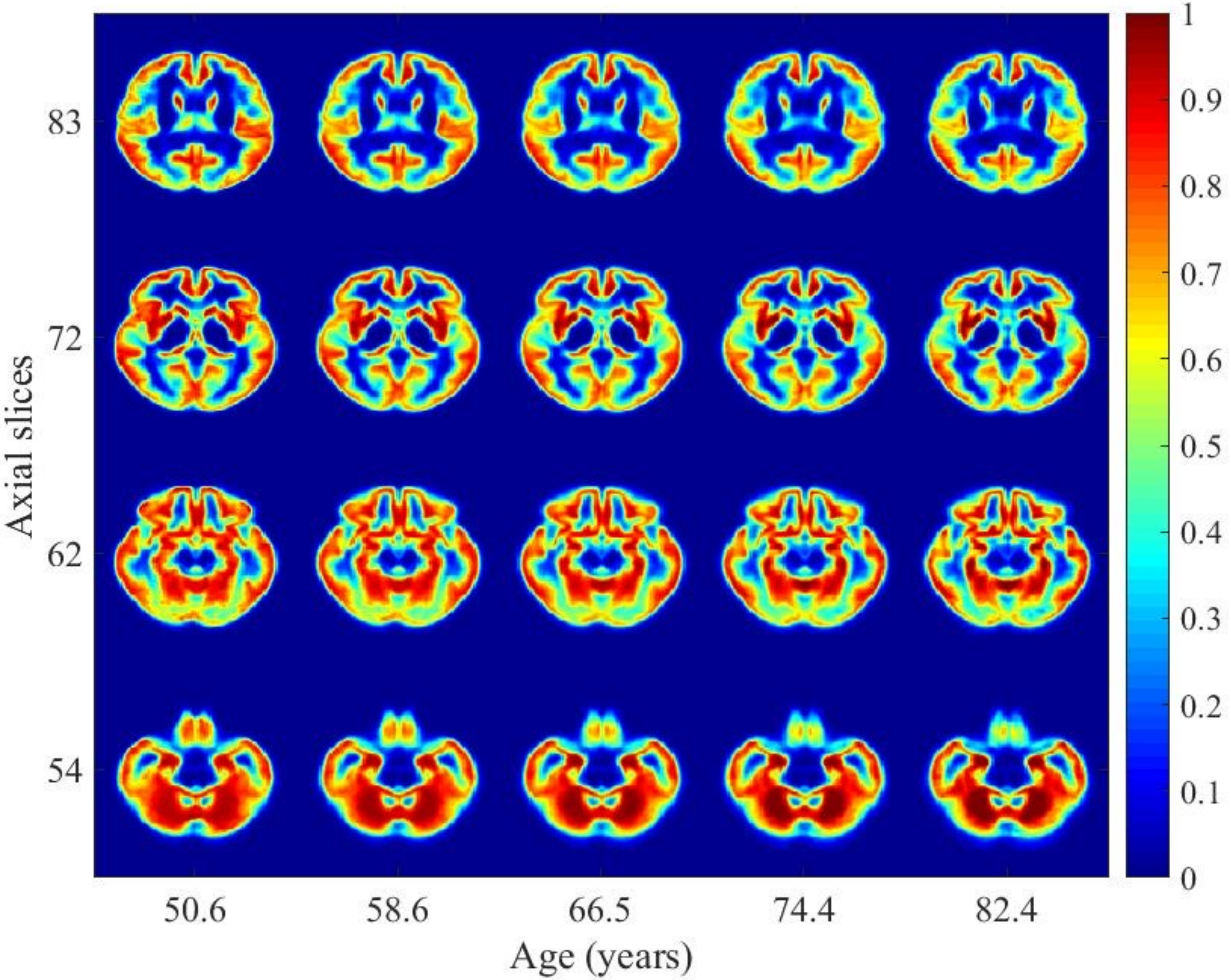

Example: Can we model the dependency between myosin and actin in neutrophils?

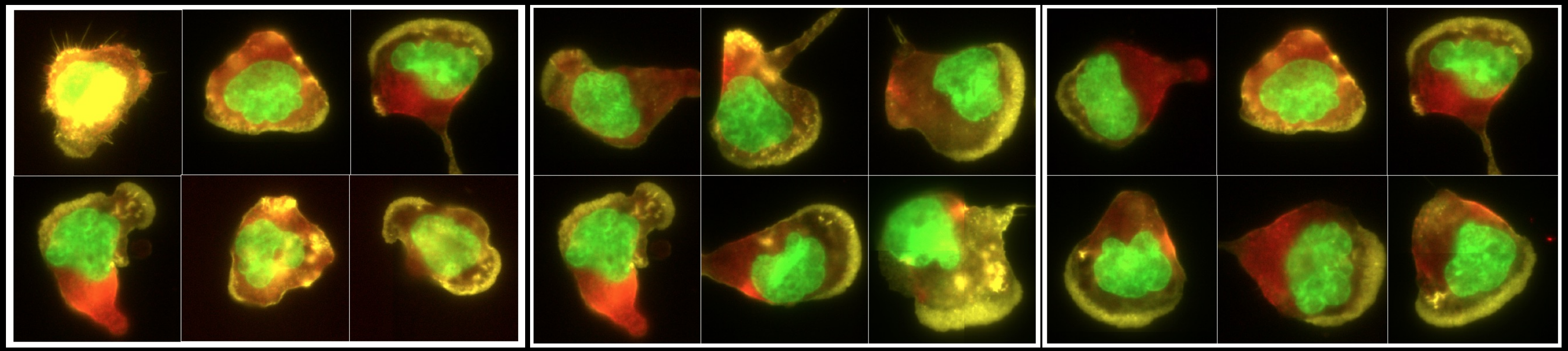

Courtesy: Theriot Lab (Stanford)

Solution:

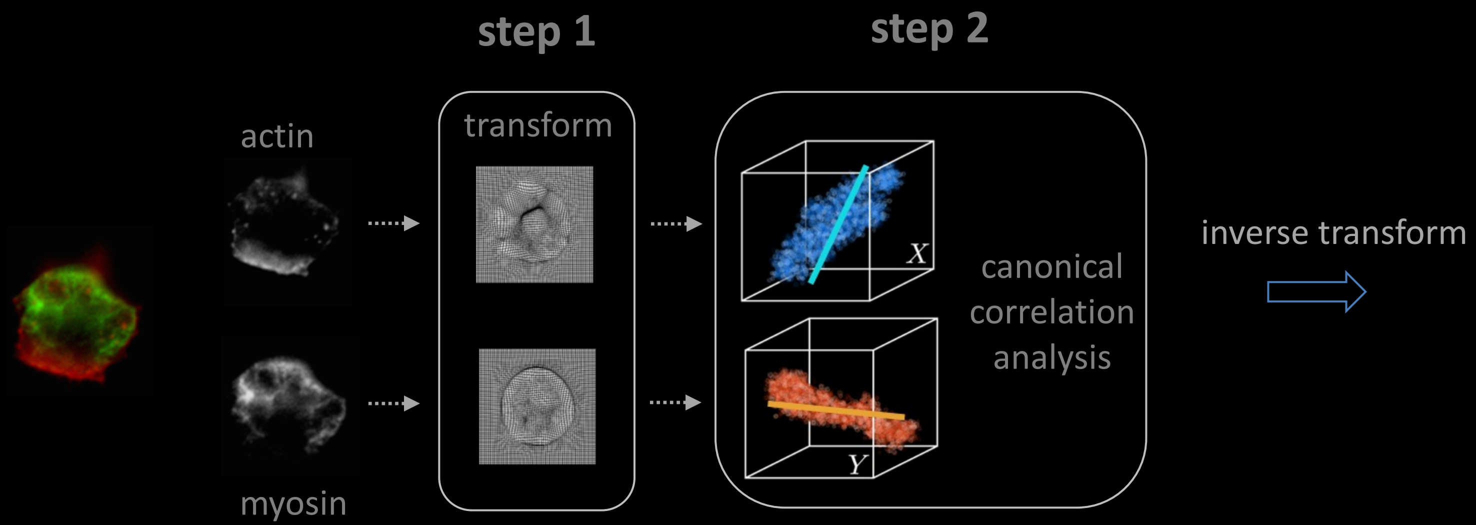

Result: Antipodal relationship between actin and myosin

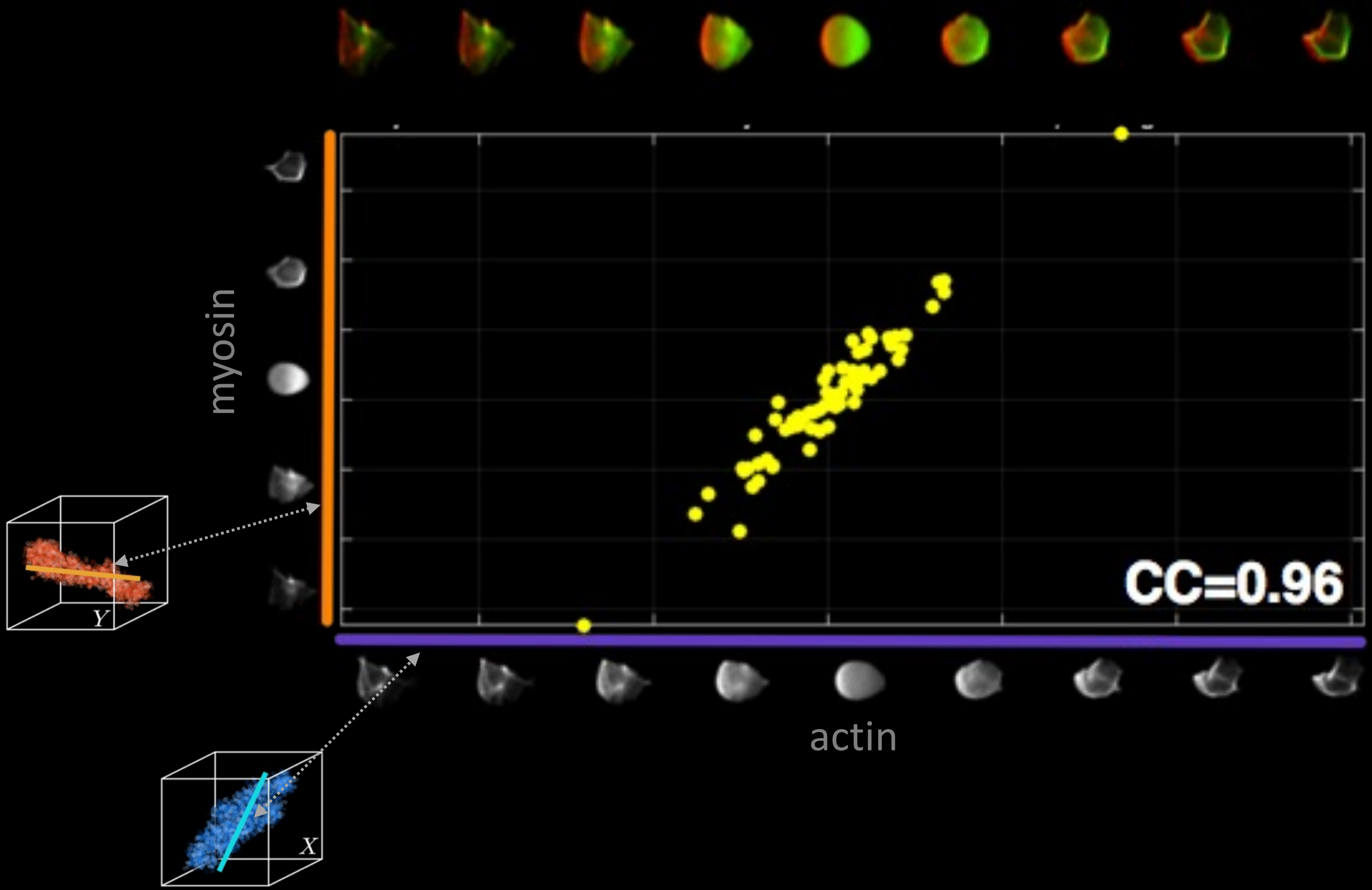

Forkhead protein translocation (drug screening)

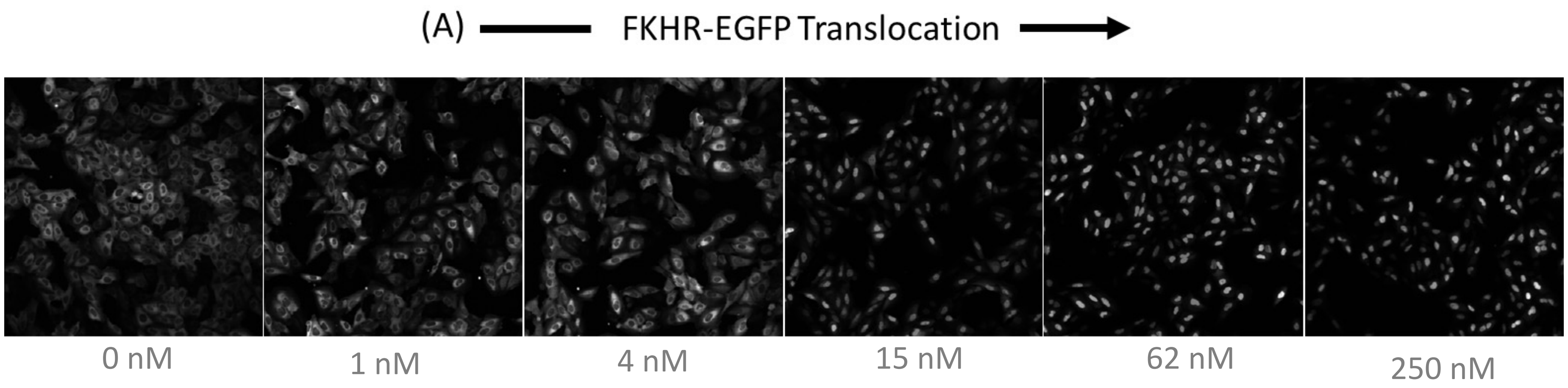

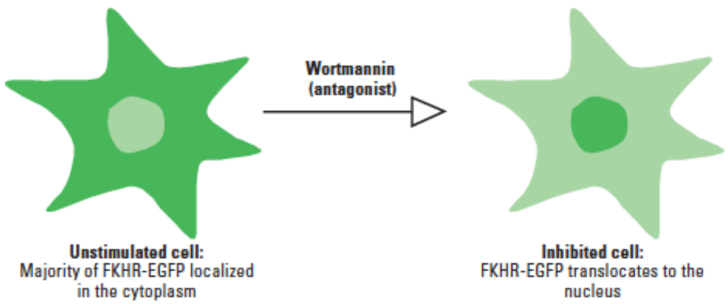

Problem statement

Can we automatically “decode” the effects of Worthamin concentration?

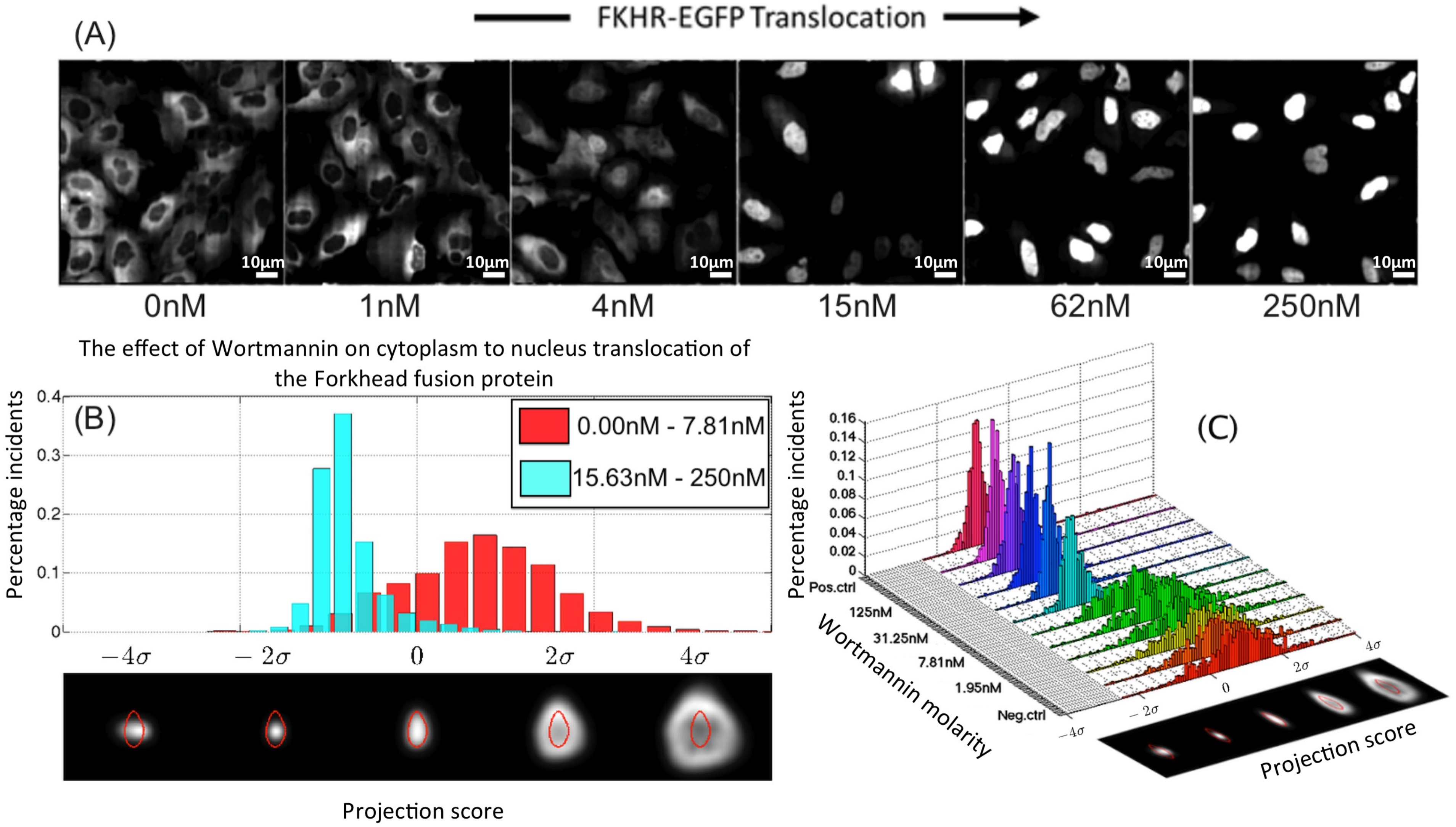
(A)
FKHR-EGFP Translocation
10µm
0nM
1nM
4nM
15nM
62nM
250nM
The effect of Wortmannin on cytoplasm to nucleus translocation of the Forkhead fusion protein
(B)
Percentage incidents
0.00nM - 7.81nM
15.63nM - 250nM
-4σ
-2σ
0
2σ
4σ
Projection score
(C)
Percentage incidents
Pos.ctrl
125nM
31.25nM
7.81nM
1.95nM
Neg.ctrl
Wortmannin molarity
Projection score

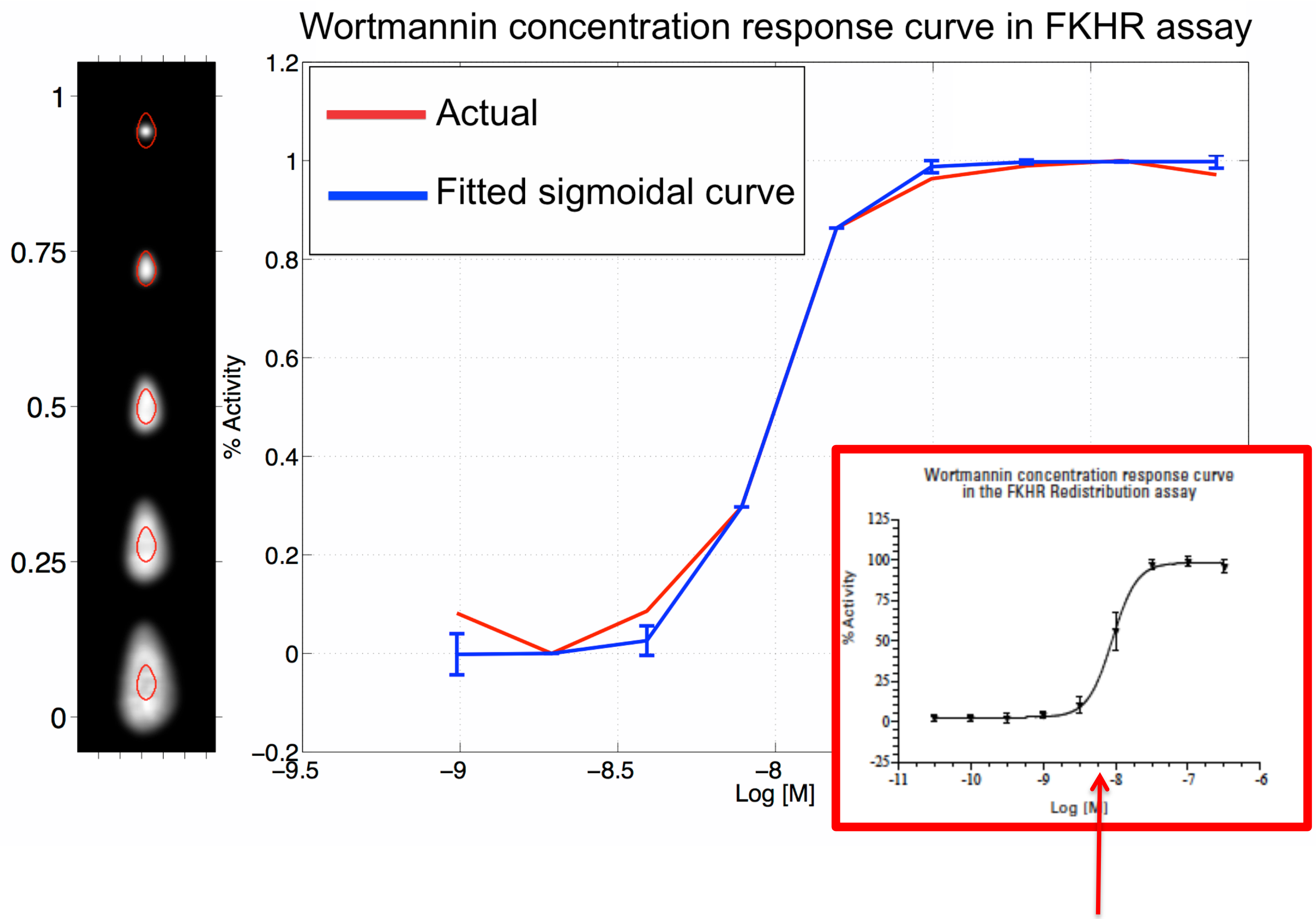

Basu, Kolouri, Rohde, PNAS 2014

From Theromo-Fisher